The Maximum Potential Intensity of Tropical Cyclones

GREG J. HOLLAND

Bureau of Meteorology Research Centre, Melbourne, Australia

(Manuscript received 28 November 1994, in final form 26 February 1997)

ABSTRACT

A thermodynamic approach to estimating maximum potential intensity (MPI) of tropical cyclones is described and compared with observations and previous studies. The approach requires an atmospheric temperature sounding, SST, and surface pressure; includes the oceanic feedback of increasing moist entropy associated with falling surface pressure over a steady SST; and explicitly incorporates a cloudy eyewall and a clear eye. Energetically consistent, analytic solutions exist for all known atmospheric conditions. The method is straightforward to apply and is applicable to operational analyses and numerical model forecasts, including climate model simulations.

The derived MPI is highly sensitive to the surface relative humidity under the eyewall, to the height of the warm core, and to transient changes of ocean surface temperature. The role of the ocean is to initially contribute to the establishment of the ambient environment suitable for cyclone development, then to provide the additional energy required for development of an intense cyclone. The major limiting factor on cyclone intensity is the height and amplitude of the warm core that can develop; this is closely linked to the height to which eyewall clouds can reach, which is related to the level of moist entropy that can be achieved from ocean interactions under the eyewall. Moist ascent provides almost all the warming above 200 hPa throughout the cyclone core, including the eye, where warm temperatures are derived by inward advection and detrainment mixing from the eyewall. The clear eye contributes roughly half the total warming below 300 hPa and produces a less intense cyclone than could be achieved by purely saturated moist processes.

There are necessarily several simplifications incorporated to arrive at a tractable solution, the consequences of which are discussed in detail. Nevertheless, application of the method indicates very close agreement with observations. For SST < 26°C there is generally insufficient energy for development. From 26° to 28°C SST the ambient atmosphere warms sharply in the lower troposphere and cools near the tropopause, but with little change in midlevels. The result is a rapid increase of MPI of about 30 hPa °C^{-1}. At higher SST, the atmospheric destabilization ceases and the rate of increase of MPI is reduced.

1. Introduction

A thermodynamical approach to the maximum potential intensity (MPI) of tropical cyclones assumes that the detailed cyclone dynamics and internal processes provide no constraint on the maximum achievable intensity. The MPI is therefore estimated from the available thermodynamic energy in the environment, including the ocean.

It is well known that for hydrostatic balance, a net warming of an atmospheric column will be accompanied by a drop in the surface pressure (see Hirschberg and Fritsch 1993 and related papers for a recent discussion). However, direct warming from the release of all the latent-heat energy in a localized region of the tropical atmosphere can reduce the surface pressure by only approximately 20–40 hPa (e.g., Riehl 1948, 1954). Intense tropical cyclones must obtain additional energy to generate the observed large pressure fall and high winds. Some of this energy arises from increased relative humidity under the eyewall, but a large part is obtained by ocean–atmosphere interaction as the surface pressures fall over a constant ocean temperature (Byers 1944; Riehl 1948, 1954; Kleinschmidt 1951; Malkus and Riehl 1960; Emanuel 1986). The moist entropy, as expressed by equivalent potential temperature, is a function of pressure and temperature. Thus, lowering the surface pressure while maintaining the ocean surface temperature leads to an increase of θ_E, which is redistributed aloft to further warm the column and lower the surface pressure, and so on.

Previous studies have estimated the MPI based on a parameterization of eye-region subsidence (Miller 1958), on calculation along parcel trajectories of the available energy to balance surface momentum losses (Malkus and Riehl 1960), on assumption of slantwise convective neutrality leading to a thermodynamically defined outflow (Emanuel 1986), and on assumption that a cyclone acts as a classic Carnot heat engine (Kleinschmidt 1951; Emanuel 1987, 1991). Except for Miller, these studies have combined dynamics and thermody-

Corresponding author address: Dr. Greg J. Holland, Bureau of Meteorology Research Center, GPO Box 1289K, Melbourne, Victoria 3001, Australia.
E-mail: holland@tom.av.gov

TABLE 1. Summary of approaches to thermodynamic modeling of tropical cyclones.

Model	Eye	Eyewall	Environment	Surface
Miller (1958): thermodynamic, based on eye subsidence.	Subsidence from θ_{ES} equilibrium level; empirical entrainment; hydrostatic P_S.	Not included directly.	Mean sounding of Jordan (1957).	T_S = SST, RH = 85%, P_{env} = 1010 hPa, $\theta_{ES} \neq p_s$.
Malkus and Riehl (1960): thermodynamics derived from dynamics, based on inflow trajectories at surface.	Not explicitly included.	Moist adiabat, $\theta_E = \theta_{ES}$, P_S hydrostatic.	Mean sounding of Jordan (1957), parameter values at r_{env}.	T_S = SST − 2, selected constant inflow angle, RH calculated, P_S calculated dynamically, $\theta_{ES} \propto p_S$.
Emanuel (1991); Carnot heat engine.	Assumed cloud filled at RH = 100%	Ascent occurs at cyclone center.	T_{out} and surface parameter values at r_{env}.	T_S = SST, RH_{env} = 75%, RH_c = 100% $\theta_{ES} \propto p_S$.
This study: thermodynamic limits on P_c	Constant θ_E, with RH defined by eye-wall mixing following Miller (1958); P_S hydrostatic	Moist adiabat, $\theta_E = \theta_{ES}$, P_S hydrostatic.	Sounding, P_{Senv}.	T_S = SST − 1, RH variable, standard 90% at eyewall, $\theta_{ES} \propto P_S$.

namics in making the assessment, although the dynamical contribution to Emanuel's result is small.

In this study we define MPI by the central pressure of a cyclone and use published empirical relationships to estimate the maximum winds for a given central pressure. We derive a new method of estimating the maximum possible pressure fall at the surface from purely thermodynamic considerations, based on hydrostatic balance with a saturated eyewall and a parameterized eye region. Haurwitz (1935) showed that hydrostatic balance required that a tropical cyclone warm core extend through the depth of the troposphere. The hydrostatic pressure fall has a nonlinear dependence on the height of an imposed warming and 70%–80% of the pressure fall in typical tropical cyclones arises from entropy changes above 500 hPa (Malkus and Riehl 1960). We show that the ability to establish such an upper-tropospheric warm core, especially in the eyewall, is the major factor in tropical cyclone intensification and determines whether a tropical cyclone can form.

The following section examines existing thermodynamic models of tropical cyclones and includes a detailed sensitivity analysis of the Carnot cycle approach suggested by Emanuel (1987, 1991). Section 3 presents our thermodynamic method, its physical basis, an energy budget, example applications, and a sensitivity analysis. A comprehensive application of the method to observed conditions is provided in section 4 and our overall findings are summarized in section 5. All terms used are defined in the appendix.

2. Existing thermodynamic models of tropical cyclones

a. Thermodynamic/dynamic models

Previous models of tropical cyclone intensity have been proposed by Kleinschmidt (1951), Miller (1958), Malkus and Riehl (1960), and Emanuel (1986, 1987, 1991). Some of their components are summarized in Table 1 and described below.

Miller (1958) noted that hydrostatic balance required that the MPI be related to the highest achievable temperature anomalies in the eye. He suggested that this maximum warming could be directly related to the degree of subsidence warming in the eye, which was determined by the moist entropy of the surface air in the eyewall; the prevailing lapse rates in the surrounding environment; the level aloft at which eyewall air is detrained to subside in the eye; and the degree of mixing between the saturated air in the eyewall and the dry subsiding air in the eye. Empirical evidence was used to determine the relative proportions of these parameters to arrive at a relationship between SST and MPI.

Malkus and Riehl (1960) examined the energetics of air parcels spiralling into the tropical cyclone near the ocean surface. While their main concern was with the dynamics of these trajectories in relationship to the available thermodynamic energy and loss of kinetic energy from dissipation at the surface, they arrived at the important conclusion that the vertical redistribution of moist entropy near the surface in convective clouds could lead to substantial pressure falls, without the requirement of subsidence per se. Thus, not all of the pressure fall in a tropical cyclone is due to eye subsidence. Malkus and Riehl also extended the findings of Riehl (1948, 1954) and Byers (1944) that the increase of moist entropy by lowering surface pressure over a constant SST was the major source of energy for tropical cyclones, to provide the relationship

$$\delta P_S = c\delta\theta_{ES}$$
$$c = -2.5, \quad (1)$$

where P_S is the surface pressure change underneath the

eyewall arising from an increase, $\delta\theta_{ES}$, in moist entropy.[1] This relationship implicitly assumes a tropopause height of around 100 hPa.

Emanuel (1986) extended the Malkus and Riehl approach to derive a relationship between central pressure and environmental parameters by assuming that the air rose along slanting moist-neutral angular momentum surfaces extending outward in the outflow layer. The cyclone was assumed to be axisymmetric and in hydrostatic and gradient balance. The only sources of energy were the addition of moist entropy in the surface inflow and radiational cooling of the outflow, and dissipation was confined to the boundary layer and the far outflow regime. This represents a Carnot heat engine cycle in which energy is added at the warm ocean surface and lost in the cool outflow, in a quite similar manner to that proposed by Kleinschmidt (1951, see also Gray 1994). An alternative Carnot cycle derivation of central pressure by Emanuel was found to be equivalent to the above integration but without the balance requirements.

Subsequent papers (Emanuel 1987, 1991) refined the model and introduced additional effects of moist thermodynamics. We shall use the approximate relationship from Emanuel (1991):

$$\begin{aligned}
\mathrm{MPI} &= P_{\mathrm{env}} e^{-X},\\
X &= \frac{\epsilon T_s \Delta S_{\max} - \dfrac{f^2 r_{\mathrm{env}}^2}{4}}{R_d T_s},\\
\epsilon &= \frac{T_s - T_{\mathrm{out}}}{T_s},\\
T_s \Delta S_{\max} &= R_d T_s \ln\frac{P_{\mathrm{env}}}{P_c} + L_v(q_c^* - q_{\mathrm{env}}),\\
q_c^* &= \frac{3.802}{P_c}\exp\left[\frac{17.67(T_s - 273.15)}{T_s - 29.65}\right], \qquad (2)
\end{aligned}$$

where the terms are defined in the appendix. The first term in the exponent, X, is the available energy for work arising from the difference of entropy between the environment and the storm center modified by the thermodynamic efficiency ϵ. The second term ($f^2 r_{\mathrm{env}}^2/4$) indicates that the energy available to lower the central pressure is reduced by that required to develop the upper anticyclone.

This relationship implies that the MPI of a tropical cyclone is determined entirely by the storm radius r_{env} at which environmental parameters of sea-level pressure P_{env}, SST, and relative humidity are defined, and the temperature of out-flowing air aloft, T_{out}. The following assumptions have been made. Dissipation only occurs in the boundary layer and at large distance in the outflow layer, so that absolute angular momentum, water substance, and entropy are conserved along streamlines; the surface temperature T_S is equal to the ocean surface temperature, which is constant at some environmental value; the environmental sounding can be approximated by an assumed moist-neutral profile; and ascent occurs at the center of the cyclone, which is saturated. Ice dynamics, together with the effects of water loading and water vapor on atmospheric density are generally neglected but with little net effect (Emanuel 1987). There also seems to be small sensitivity to the incorrect assumption of a closed Carnot cycle for tropical cyclones. The assumed environmental RH and surface temperature are required to specify a full atmospheric sounding based on Emanuel's concept of moist neutrality. This, together with the lack of an eye and the arbitrary choice of 100% surface relative humidity in a cloud-filled cyclone core are the major limitations on application of this model.

b. *Sensitivity of existing thermodynamic models to control parameters*

The main parameters in Miller's (1958) method of estimating MPI are the degree of entrainment from the eyewall to the eye and the choice of surface moist entropy. Miller's entrainment is directly related to the relative humidity of the eye, and we show in section 3f that there is little sensitivity to the choice of realistic values for eye humidity. However, while Miller was aware of the requirement for additional moist entropy from the ocean surface during intensification of a tropical cyclone, he chose to disregard this. Instead, the surface equivalent potential temperature was derived from the SST at the environmental pressure, with an assumed constant surface relative humidity of 85%. It is now well known that the air–sea interaction cycle is crucial to tropical cyclone intensification (Byers 1944; Kleinschmidt 1951; Malkus and Riehl 1960; Emanuel 1986, 1987, 1991). We also show in later sections that the derivation of MPI is very sensitive to small changes in the assumed surface relative humidity.

In deriving Eq. (1), Malkus and Riehl (1960) assumed only that the slope of the eyewall was nearly perpendicular, so that the contribution of dry adiabatic subsidence to density gradients in the rain area was negligible, and that the level of zero pressure perturbation for hydrostatic calculations was 100 hPa. Their relationship provides an indication of the pressure fall from vertical redistribution of increasing surface moist entropy. However, they assumed a static relationship that did not take into account the associated fall in surface pressure and the feedback to increased moist entropy. The thermodynamic approach in section 3 indicates that the empirical constant c in Eq. (1) is a strong function of surface pressure.

Of the control parameters in the Carnot model approach, the series of papers summarized by Emanuel

[1] All terms used in this paper are defined in the appendix.

TABLE 2. Sensitivity of the MPI predicted by the Carnot cycle of Emanuel (1991) to defined parameters.

Parameter	Standard value	Range	MPI range hPa
r_{env}	500 km	50–1100 km	20
P_{env}	1015 hPa	1000–1020 hPa	25 1.2 hPa/hPa
RH_{env}	75%	70%–90%	130 6.2 hPa/%
RH_c	100%	80%–100%	130 −6.2 hPa/%
SST	30°C	20°–31°C	115 10.5 hPa/°C
T_{out}	−75°C	−60 to −90°C	120 −4 hPa/°C

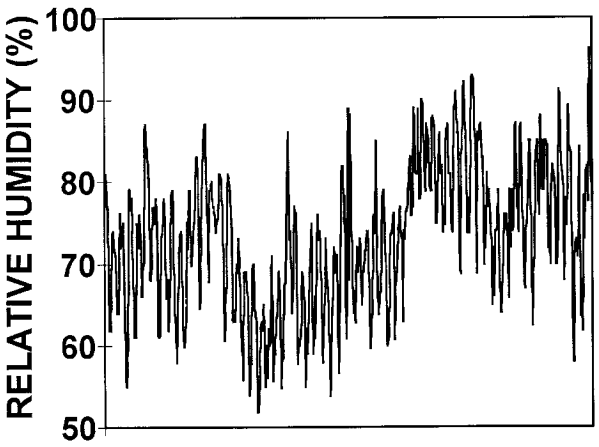

FIG. 1. Variation of surface relative humidity at Willis Island (a small coral cay, 500 km off the northeast Australian coast) for 3-h observations during January and February 1992.

(1991) have extensively addressed the sensitivity to SST and outflow temperature and have noted, though not described in detail, the sensitivity to environmental humidity. Because of the widespread use of Emanuel's model in estimating the MPI, we examine the sensitivity to all control parameters.

Table 2 indicates the degree of sensitivity relative to the standard MPI of 862 hPa (indicated by the star in Fig. 2 of Emanuel 1991) for the parameter values shown in the left-hand column. The parameter ranges were determined by the following reasoning. We choose the SST range of 20°–31°C as being reasonable for significant tropical cyclones (e.g., Merrill 1988). The summer tropopause temperatures at Australian region stations vary from less than −80°C in the deep Tropics to −65°C near the edge of the cyclone region. The lowest observed cloud-top temperature in tropical cyclones is −102°C (Ebert and Holland 1992), but this would not have been representative of the whole outflow regime. We therefore choose an outflow temperature range of −60° to −90°C. If r_{env} is taken as the radius of outer closed isobar or gale force winds, then observed values range from 50 to 1100 km (Holland 1993). Environmental pressures experienced by tropical cyclones vary from above 1020 hPa in the subtropical ridge to below 1000 hPa in the monsoon trough. Environmental humidity values can range from below 70% to 90%, as indicated in Fig. 1 by the series of 3-h observations from Willis Island, a small coral cay 500 km off the northeast Australian coast (Table 3). The choice of 100% RH in the cyclone eye gives the maximum achievable pressure fall for given environmental parameters, but the choice is arbitrary and has not been observed in tropical cyclones. We therefore choose a range from the 80% observed in the eye of Tropical Cyclone Kerry (Black and Holland 1995) to the 100% used by Emanuel.

The Emanuel approach is markedly sensitive to the choice of environmental and central relative humidities. For the intense cyclone example used here, a 2% change of relative humidity produces the same MPI variation as a SST change of 1°C. The monthly means at Willis Island (Fig. 1) for the peak cyclone months of January and February 1992 were 69% and 77%, respectively, implying a 50-hPa variation of potential intensity. No observational evidence has been produced to indicate that this substantial variation of relative humidity over tropical oceans equates to similar sensitivity in cyclone intensity. There also are no observations of the remarkably high θ_E values that result from the assumption of 100% RH in the cyclone core. For example, in Supertyphoon Flo application of 100% relative humidity to the observed SST of 29.9°C and central pressure of 891 hPa suggests θ_E near 408 K, which is much higher than the observed maximum values of 384 K (section 4a, and Merrill and Velden 1996).

3. Thermodynamic limitations on maximum potential intensity (MPI)

The thermodynamic limitations on tropical cyclone intensity are reexamined using an alternative thermodynamic approach to those described in the previous section. As indicated by Fig. 2, the method explicitly includes an environment, an eyewall, and an eye. We make no assumptions on how air parcels converge toward or away from the cyclone center; our only interest is in the property of the surface air that has arrived underneath the eyewall, regardless of where it has come from. The following assumptions are made.

TABLE 3. Upper-air sounding stations used in this study.

Station	Latitude	Longitude	SST range (°C)
Barbados	13 N	59 W	26.8–28.6
Bermuda	33 N	64 W	19.3–27.7
Guam	13 N	145 E	27.3–29.2
Miami	26 N	80 W	23.5–29.4
Willis Island, Australia	16 S	150 E	25.8–29.4

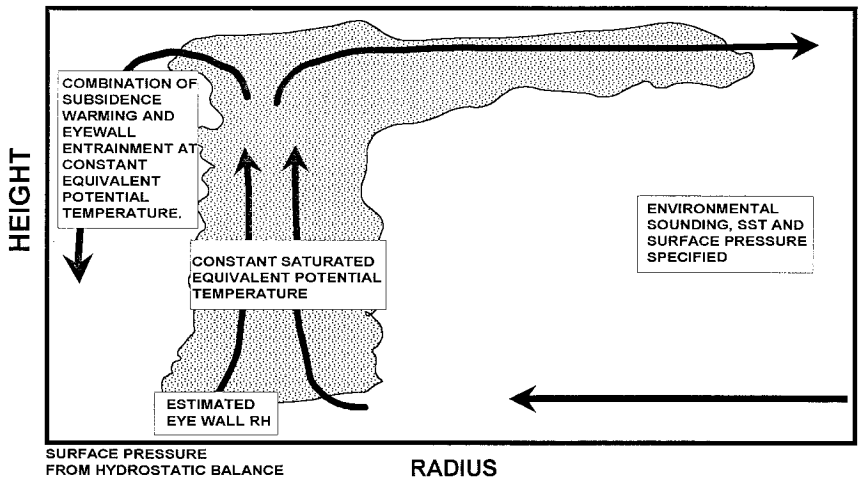

FIG. 2. Schematic of the basic components of the thermodynamic approach to estimating MPI.

1) The environment can be represented by a single sounding, $T_{\text{env}}(p)$, surface pressure, P_{env}, and surface air temperature, T_S.
2) The cyclone is essentially symmetric, and intense systems include a vertical eyewall in which the saturated equivalent potential temperature is constant with height surrounding an eye with constant equivalent potential temperature, which is set at the maximum achievable at the surface under the inner edge of the eyewall. The effects of outer cloud regions are neglected.
3) The surface pressure drop from the environment is defined hydrostatically by the temperature anomaly in the column above, with the level of zero pressure perturbation being defined by the level of convective equilibrium.
4) The temperature anomaly in the eyewall, or general cloudy region for weak systems, results from moist adiabatic lifting of surface air aloft; additional warming in the eye results from subsidence with entrainment from the eyewall, subject to the constraints in (2).
5) We neglect ice-phase processes and entrainment of midlevel air from outside into the eyewall (these two processes are to some extent self-cancelling).

Estimates are required for the surface relative humidity under the eyewall and the degree of entrainment of saturated eyewall air into the eye. We do not explicitly include the impact that spray and rainfall has on the surface energy budget (Fairall et al. 1994). This aspect is discussed in section 3f.

a. Method

The components of the method are indicated in Fig. 2 and the iterative solution, outlined in Fig. 3, consists of three parts:

1) The surface pressure response to an initial redistribution of all available moist energy at the assumed surface relative humidity;
2) An iterative process to utilize all energy available from the feedback between the developing tropical cyclone and the ocean in the inner eyewall region; and
3) For systems that become sufficiently intense (at least 20 hPa below ambient pressure), inclusion of an eye with constant equivalent potential temperature defined by that at the ocean surface under the eyewall. Details of the required subsiding air and eyewall entrainment are thus implicit.

Since the conventional formula for θ_E can give errors of several kelvin in the humid Tropics, we use the empirical formulation derived by Bolton (1980):

$$\theta_E = \theta \exp\left[1000q(1 + 0.81q)\left(\frac{3.376}{T_L} - 0.00254\right)\right], \tag{3}$$

where T, q, and p are evaluated at the initial level, with mixing ratio given by

$$q = \frac{\text{RH}}{100}q^*,$$

$$q^* = \frac{3.802}{p}\exp\left[\frac{17.67(T - 273.15)}{T - 29.65}\right]. \tag{4}$$

Here T_L is the temperature at the lifting condensation level and e is vapor pressure defined by

$$T_L = \frac{2840}{3.5\ \ln T - \ln e - 4.805} + 55,$$

$$e = \frac{pq}{0.622 + q}. \tag{5}$$

At the eyewall we assume that the surface equivalent potential temperature θ_{ES} is defined by the surface air

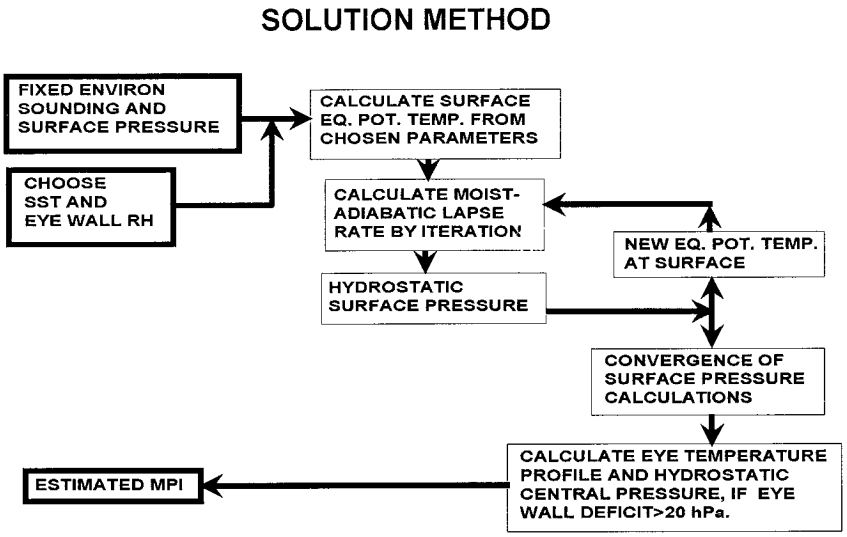

FIG. 3. Flow chart describing the solution method for estimating the MPI.

temperature T_S and mixing ratio q_S, and no regard is taken of the origin of the surface air parcels. The temperature anomaly in the eyewall, $\Delta T_{\text{eyewall}}$, is then found by using a saturated column with constant $\theta^*_{EC} = \theta_{ES}$ with height. This is solved iteratively for T, from

$$\Delta T_{\text{eyewall}}(p) = \frac{\theta^*_{EC}\left(\dfrac{p}{1000}\right)^{R_d/c_p}}{\exp\left[1000q^*(1 + 0.81q^*)\left(\dfrac{3.376}{T} - 0.00254\right)\right]} - T_{\text{env}}(p). \quad (6)$$

The hydrostatic change in surface pressure associated with warming aloft (Hirschberg and Fritsch 1993) is

$$\Delta P_s = \frac{P_s}{T_v(P_s)} \int_{P_s}^{P_T} \Delta T_v \, d \ln p,$$

$$T_v = T(1 + 0.61q). \quad (7)$$

The appropriate choice of P_T for general use has been subject of some recent debate (Hirschberg and Fritsch 1993). In the case of an intense cyclone, the level of changeover from cyclonic to anticyclonic flow and the level of zero buoyancy are roughly similar. We therefore adopt a pragmatic choice of P_T as the level at which a saturated moist adiabat from the lifting condensation level in the eyewall region crosses the environmental profile. This approach errs on the side of higher intensity, since some cyclones can have eyewall cloud penetrating the stratosphere (e.g., Ebert and Holland 1992), with resultant cooling and cyclonic flow farther aloft.

Since θ_{ES} and P_S are functions of each other, pressure falls lead to increased θ_{ES} and hence to further pressure falls, etc. This is the air–sea interaction by which tropical cyclones extract much of their energy from the ocean (Riehl 1948, 1954; Malkus and Riehl 1960; Emanuel 1986). Fortunately, the process converges for all physically realizable conditions (section 3f) to give an estimate of the maximum achievable pressure drop to the eyewall. This pressure drop is obtained by the iterative procedure in Fig. 3, which is quite straightforward: initially the pressure fall is calculated from warming following adjustment of the environmental sounding to a moist adiabat defined by θ_{ES}, then this is used to update the surface θ_{ES}, which is then redistributed to give another pressure fall, and so on. Convergence is assumed once the surface pressure is changing by less than 1 hPa. This iterative process includes both the effects of surface moist entropy exchanges at reduced pressure and constant temperature, and the atmospheric stabilization arising from increased warming aloft.

The cyclone eye is parameterized in the following fashion. If the calculated eyewall pressure drop is less than 20 hPa, or if there is insufficient potential energy (section 3d), the center of the cyclone is assumed to be full of moist, cloudy air and all pressure falls result from redistribution of moist entropy aloft. This is representative of tropical depressions and weak tropical cyclones. Observations (Dvorak 1975, 1984) indicate that an eye develops once a tropical cyclone develops to near hurricane strength, parameterized here by a pressure fall of greater than 20 hPa in the cloud region.

There are conflicting views of the dynamics of a tropical cyclone eye, which vary from a stagnant pool of air that has subsided only a few kilometers along a dry adiabat (Malkus 1958; H. Willoughby 1995, personal communication) to a system that is rapidly ventilated

by inward advection aloft and lower-level mixing across the eyewall (Miller 1958). We adopt an approach to estimating an eye sounding that is consistent with either concept. We assume that the eye is characterized by subsiding air, which has inward mixing of eyewall air and upward mixing of surface air in proportions that increase towards the surface. The maximum entropy available to the eye is that originating at the ocean surface under the inner edge of the eyewall. The lack of contribution by stratospheric air is discussed later.

Thus, both the eye and eyewall are constrained by a maximum equivalent potential temperature given by

$$\theta_{E,\text{eye}} = \theta_{ES}$$
$$\theta_{EC} = \theta_{ES}. \tag{8}$$

This assumption removes any need for us to define the details of the subsidence and horizontal entrainment that is required to maintain the eye, since any combination of these will lead to the same result. The approximately constant nature of θ_E in the eye is confirmed by both observations (Hawkins and Rubsam 1968; Jorgensen 1984b; Frank 1984) and numerical modeling results (e.g., Bender et al. 1993).

Derivation of the eye temperature structure requires an estimate of the relative humidity in the eye. Observations of humidity soundings throughout the full eye in intense cyclones are rare, but all indicate a relatively dry upper core with an inversion near 700 hPa, below which high humidity prevails. After experimentation with a wide range of potential parameterizations, including those by Malkus (1958) and Miller (1958), we settled on use of a relatively simple scheme that is constrained and adjusted by the cyclone energy budget. The relative humidity in the eye is assumed to take the form

$$\text{RH} = \begin{cases} 0, & P \le 200 \text{ hPa} \\ \max(X, 0), & 200 < P \le 450 \text{ hPa} \\ \min(X, 80), & 450 < P \le 700 \text{ hPa}, \end{cases} \tag{9}$$

where

$$X = C + \frac{(P_{\text{S,eyewall}} - 800)(P - 200)}{1000}. \tag{10}$$

Here, $C = -10$ but is allowed to vary between 0 and -20 to ensure that the buoyant potential energy of the eye is slightly less than the available energy from the oceanic feedback (section 3d). Below 700 hPa, the relative humidity increases linearly to 95% at 900 hPa.

The temperature anomaly in the eye is then given by

$$\Delta T_{\text{eye}}(p) = \frac{\theta_{ES}\left(\dfrac{p}{1000}\right)^{R_d/c_p}}{\exp\left[1000q^*(1 + 0.81q)\left(\dfrac{3.376}{T} - 0.00254\right)\right]} - T_{\text{env}}(p), \tag{11}$$

where q is obtained from Eq. (4) with the specified humidity. The eye temperatures derived from this approach tend to be maximum around 300–400 hPa, which is substantially lower than the upper-troposphere maximum that is derived by the assumption of a saturated eye in Emanuel (1991). Applying this temperature anomaly to Eq. (7) gives the maximum achievable pressure fall ΔP_{Smax} and finally

$$\text{MPI} = P_{\text{Senv}} - \Delta P_{\text{Smax}}. \tag{12}$$

b. A standard set of parameters

The environment is defined by an actual sounding, with surface temperature and pressure. Where the surface temperature is not known, T_{Senv} is assumed to be 1°C cooler than the SST (e.g., Pudov and Petrichenko 1988). If the surface pressure is not known, P_{Senv} is set to the monthly mean for the basin, which is consistent with values of the outer closed isobar in tropical cyclones in the Coral Sea compared to the monthly mean pressure at Willis Island and other studies (e.g., Atkinson and Holliday 1977). We assume a surface relative humidity under the eyewall of 90%. This is within and to the high side of the range of achievable values: Malkus and Riehl (1960) obtained a value of 85% from their boundary-layer trajectory calculation; boundary-layer simulations by J. Kepert (1994, personal communication) find values ranging from 80% to 95%; and reports by aircraft reconnaissance observers indicate cloud base between 300 and 500 m in intense cyclones, which equates to 80%–90% RH.

A number of studies have empirically addressed the relationship between maximum winds and central pressure. Unfortunately, these provide no standard error estimates and tend to overemphasize the quality of the relationship. Further investigation of these relationships is warranted but beyond the scope of this study. We use the Dvorak relationship (Fig. 4) to convert the maximum wind intensities of DeMaria and Kaplan (1995) to central pressures. We also use the Atkinson and Holliday (1977) relationship

$$v_m = 3.4(p_{\text{env}} - p_c)^{0.644} \tag{13}$$

to determine the maximum winds for kinetic energy calculations.

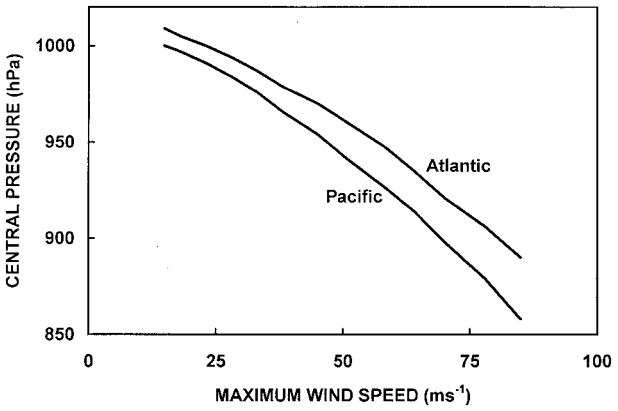

FIG. 4. The Dvorak relationship between cyclone central pressure and maximum winds (1-min mean) for the North Atlantic (Dvorak 1984) and the western North Pacific (Shewchuck and Weir 1980).

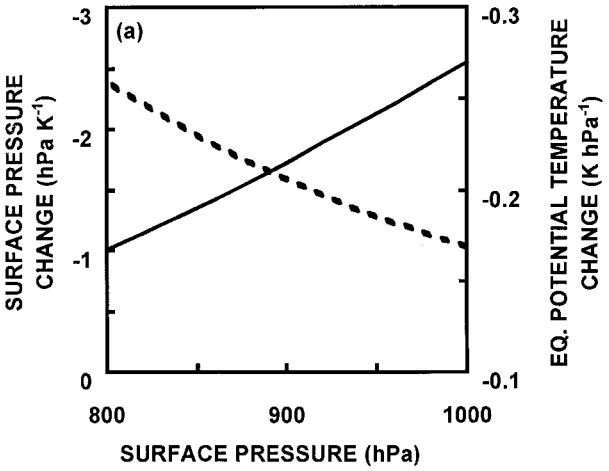

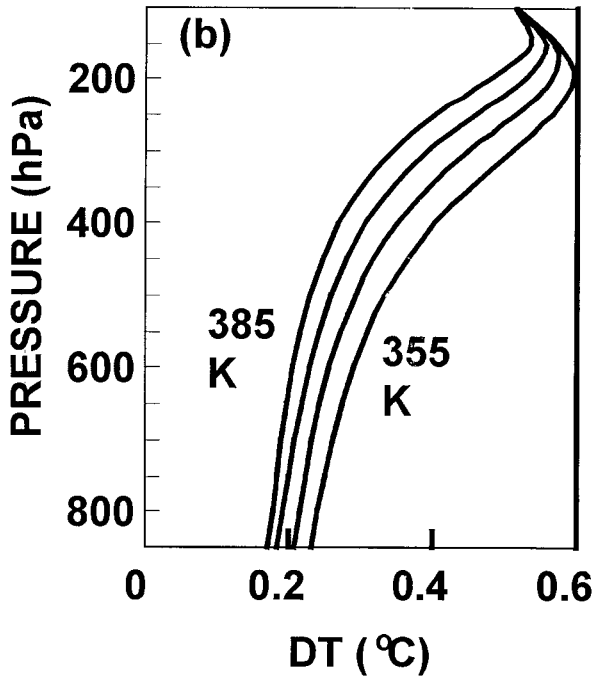

FIG. 5. Illustration of the reasons for convergence of the thermodynamic model: (a) Relative magnitudes of $\partial\theta_{ES}/\partial P_s$ (dashed line, right axis) and $\partial P_S/\partial\theta_{ES}$ (solid line, left axis) and their variation with surface pressure; (b) decreasing degree of warming between moist adiabats per K change of θ_E for θ_{ES} = 355, 365, 375, and 385 K (using Willis January sounding).

c. Physical basis

The method outlined here is based on the hypothesis that the only significant source of energy for cyclone development is the ocean surface, with the maximum contribution coming from under the inner eyewall. The eye is crucial to establishing the observed cyclone structure, but eye processes contribute no additional energy.

Initially we redistribute the preexisting surface moist entropy (at the assumed surface relative humidity) aloft in a saturated column to represent the cloud-filled region or developing eyewall of a tropical cyclone. The resultant warming produces a hydrostatic change of surface pressure (we assume that sufficient time has elapsed for the required secondary circulations and divergence patterns to develop and act). Since the surface temperature and humidity are specified, the reduction of surface pressure increases the moist entropy. Redistribution of this air aloft produces a further pressure fall, followed by higher moist entropy and further pressure falls, etc.

The surface pressure decrease at each stage converges to a limiting value for the following reasons. Since the saturation mixing ratio increases exponentially with temperature [Eq. (4)], for a constant $\Delta\theta_{ES}$ the degree of warming at any atmospheric level decreases as the temperature increases [Eq. (6), Fig. 5a]. Thus, for all physically achievable surface pressures and atmospheric conditions, there is a strong limitation on the surface pressure fall that can be achieved (Fig. 5b). The depth of the atmospheric column being warmed also decreases with falling surface pressure, but this is a relatively minor effect.

The saturated equivalent potential temperature in the eyewall produces a warming that is maximum at high levels where the atmosphere cannot hold significant moisture. Since subsidence drying has a minor effect above 250–100 hPa, almost all the high-level warming (including the eye) is derived from eyewall processes. The relative importance of inward advection and mixing of eyewall air and drying by eye subsidence is indicated by application of the model to the September Barbados (Table 3, MPI 906 hPa) sounding in Fig. 6. Also shown in Fig. 6 are the observed temperature changes for Hurricane Hilda (P_c = 945 hPa, Hawkins and Rubsam 1968), derived by assuming that the inner edge of the eyewall lay just inside the maximum winds. The model agrees well with the analysis by Hawkins and Rubsam, where the eyewall warming dominated the upper tro-

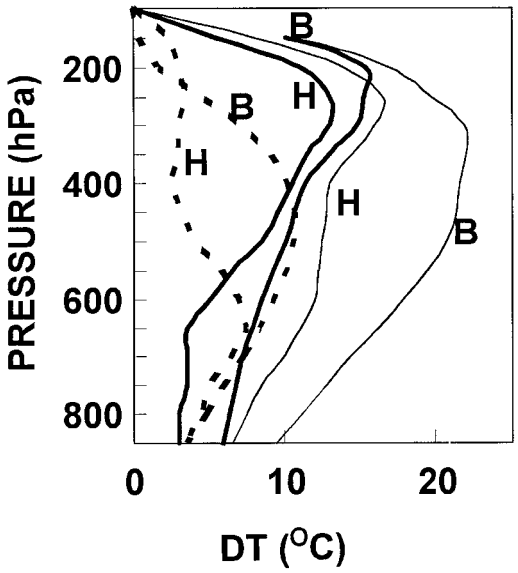

FIG. 6. Comparison of the relative warming in Hurricane Hilda (H; Hawkins and Rubsam 1968) and that derived from application of the thermodynamic model to the mean August sounding at Barbados (B). Data are normalized to the maximum temperature perturbation, light solid lines indicate the total warming in the eye, solid lines the warming at the eyewall (taken to be 1.5 × RMW for Hilda), and dashed lines are the additional warming from the eyewall to the eye.

posphere and was about equal to the eye warming in lower levels. Similar results were found by Malkus (1958) and by LaSeur and Hawkins (1963), who observed the highest upper-tropospheric temperatures in the cirrus on the inner edge of the eyewall.

Because of the greater impact of upper-level warming on pressure falls [Eq. (7)], the eyewall warming provides the major contribution to the MPI. For this model, 60%–80% of the total pressure fall from the environment occurs at the inner edge of the eyewall, which is in good agreement with observations (e.g., Holland 1980).

d. Energy budget

A detailed examination of the energetics of cyclone development are beyond the scope of this study. Emanuel (1991) and related papers discuss the energetics of the secondary circulation in the absence of any convective available potential energy (CAPE). There is significant difference of current opinion on the direct role of CAPE in cyclone development, but there is no doubt that substantial vertical motion, and hence CAPE, exists in the eyewall of some tropical cyclones (e.g., Ebert and Holland 1992; Black et al. 1994). The energetics of the eye–eyewall cycle in intense tropical cyclones has been examined by Willoughby et al. (1982), Shapiro and Willoughby (1982), and related papers. Smith (1980) also indicates that eye subsidence is a natural consequence of the decreasing cyclonic flow with height.

The energetic consistency of the model is assessed by the following approach. The total potential energy (TPE) consists of the vertically integrated difference between the environmental sounding and a moist adiabat defined by the surface temperature and assumed relative humidity at the eyewall, together with the increase energy derived by the air–sea interaction with falling surface pressures at constant surface temperature,

$$\mathrm{TPE} = g\int_{z_0}^{z_T}\frac{T_{madiab} - T_{\mathrm{env}}}{T_{\mathrm{env}}}\,dz + R_d T_{\mathrm{s}}\ln\frac{p_{\mathrm{env}}}{p_{\mathrm{eyewall}}} + L_v(q_{\mathrm{eyewall}} - q_{\mathrm{env}}). \quad (14)$$

Note that this must be reduced by the thermodynamic efficiency of the system to determine the available potential energy for work done in the cyclone development. The buoyant potential energy of the mature hurricane can be estimated by

$$\mathrm{PE} = g\int_{z_0}^{z_T}\frac{X - T_{\mathrm{env}}}{T_{\mathrm{env}}}\,dz, \quad (15)$$

where $X = T_{\mathrm{eyewall}}$ for estimating the energy available to maintain the secondary circulation and $X = T_{\mathrm{eye}}$ for the total buoyant potential energy in the cyclone. The kinetic energy is estimated by

$$\mathrm{KE} = \frac{v_{\max}^2 - v_{\mathrm{env}}^2}{2}, \quad (16)$$

where v_{env} is set to 15 m s^{-1} to represent the gale force winds at the edge of the cyclone. The frictional dissipation along the surface branch of the secondary circulation can be obtained by integration of Bernoulli's equation (e.g., Emanuel 1991) to get

$$\int_{\mathrm{env}}^{\mathrm{eyewall}}\mathbf{F}\cdot d\mathbf{l} = R_d T_{\mathrm{s}}\ln\frac{p_{\mathrm{env}}}{p_{\mathrm{eyewall}}}. \quad (17)$$

Application of Eqs. (14)–(17) to the derived values for the January mean sounding at Willis Island provides the summary shown in Fig. 7. The total potential energy from surface processes slightly exceeds that stored in the buoyant potential energy and kinetic energy of the derived tropical cyclone. The buoyant energy in the eyewall also is slightly higher than that required to offset surface frictional losses in the secondary circulation. This is consistent with the additional small energy needed to generate the anticyclonic circulation in the outflow region (Emanuel 1991). Notice that the final kinetic energy is less than 20% of the total potential energy.

The eye contributes around 30%–40% of the buoyant potential energy. Thus the work done in generating an eye is about one-third of the total potential energy from surface processes, which is indicative of the efficiency of the eye development process. This confirms that our choice of eye parameterization is consistent with the available energy for cyclone development and indicates that there is a strong limitation of the degree of undilute subsidence occurring in the eye. Simply bringing air

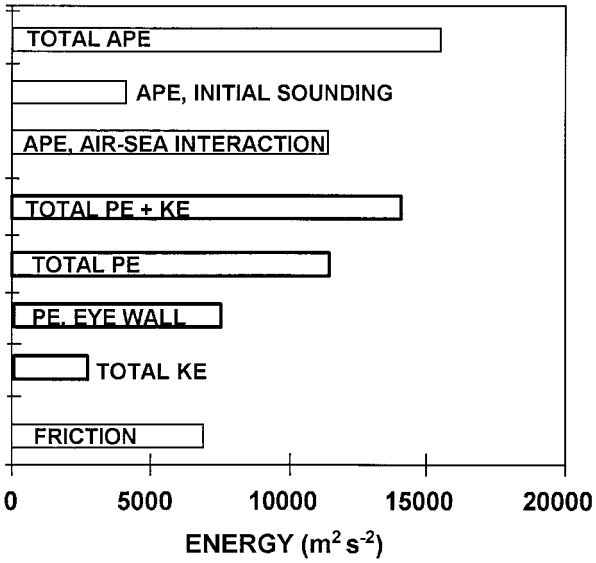

FIG. 7. Energy budget derived from application of the thermodynamic model to the January mean sounding at Willis Island. See text for discussion of terms.

adiabatically to the surface would require 50% more than the available potential energy.

An important assumption here is that there is no significant intrusion of stratospheric air into the eye. Conversion from the kinetic energy of upward motion is the only significant source of energy for this to occur in a tropical cyclone, and there seems to be insufficient sustained high eyewall vertical motion at the tropopause for significant development. Should air penetrate the stratosphere, the resulting cooling can be expected to produce a surface pressure increase under the eyewall that counters any eye subsidence effects. This reasoning is supported by the lack of stratospheric intrusions in available observations (Fig. 6, section 4) and in high-resolution numerical models (e.g., Bender et al. 1993). It also concurs with the analyses by Koteswaram (1967) and Merrill and Velden (1996) that the tropopause above tropical cyclones tends to be cooler than normal.

Transient stratospheric incursions occur in the vicinity of strong vertical motions and special upper-tropospheric wind structures (Holland et al. 1984). These may help initiate the rapid intensification sometimes associated with the growth of very intense convective cells in weak tropical cyclones (Gentry et al. 1970; P. Black 1990, personal communication).

The energy budget in Eqs. (14)–(17) was computed for all MPI derivations in this study to ensure that the available potential energy was sufficient for the derived potential and kinetic energy changes. For weaker cyclones, the energy budget provided an excellent check on our choice of both the eye parameterization and the 20-hPa minimum pressure fall for eye development.

e. An example application

We apply the method to the mean January and July soundings for Willis Island and Barbados (Table 3). The Willis Island sounding for January is indicated in Fig. 8a and the differences of the other soundings are in Fig. 8b. The environmental pressures are set at 1010 hPa for both months at Barbados and at 1007 hPa in January and 1014 hPa in July at Willis Island. The resulting MPI values in Table 4 are close to those that have been observed.

The contributions of various thermodynamical processes in establishing the central pressure are indicated in Table 4 for the summer Willis Island and Barbados soundings. Barbados in summer is slightly cooler than Willis throughout the troposphere (Fig. 8b) and has a lower and warmer tropopause. Increasing the relative humidity under the eyewall, then adjusting to a moist adiabat with constant θ_{ES} results in a significant pressure fall at both stations and indicates that a hurricane strength cyclone could develop from increased surface relative humidity, without any air–sea interaction cycle. In reality, however, the air–sea interaction will commence as soon as the surface pressures start to fall and full intensification to the observed values of MPI requires that this occur.

For a minimal hurricane, the fall of surface pressure is around 2.5 hPa for each 1 K increase of θ_{ES} in close agreement with Eq. (1) (Malkus and Riehl 1960); however, this ratio decreases to 1:1 for very intense storms (Fig. 5). Examination of Fig. 5 also indicates that convergence of the iteration is assured, as the cycle of falling surface pressure and increasing θ_E is sharply reduced as the pressure falls.

f. Sensitivity to control parameters and assumptions

We detail the sensitivity of changes of T_S and P_{env} to the depth of the eyewall, to the assumed parameters of eyewall relative humidity and eye entrainment, and to implicit assumptions, such as a vertical eyewall with constant saturated θ_E. The Willis Island January sounding (Fig. 8a) is used to specify the environment, with observed $T_{Senv} = 28.4$°C and $P_{env} = 1007$ hPa, and with $RH_{S,eyewall}$ set at 90%. The resulting relationships are all nearly linear, but of substantially different amplitudes (Table 5).

Ocean temperatures: Large variations of SST for a fixed environmental sounding are physically unrealistic, as the atmospheric sounding can reasonably be assumed to be in convective–radiative equilibrium with the general oceanic temperatures. Small SST changes of a few degrees can be expected from tropical cyclone movement over sharp temperature gradients or from oceanic cooling produced by the cyclone. The MPI response to such small SST changes for a fixed summer sounding at Willis Island is large (Table 5). Examination of other profiles (not shown) indicates that the sensitivity is high-

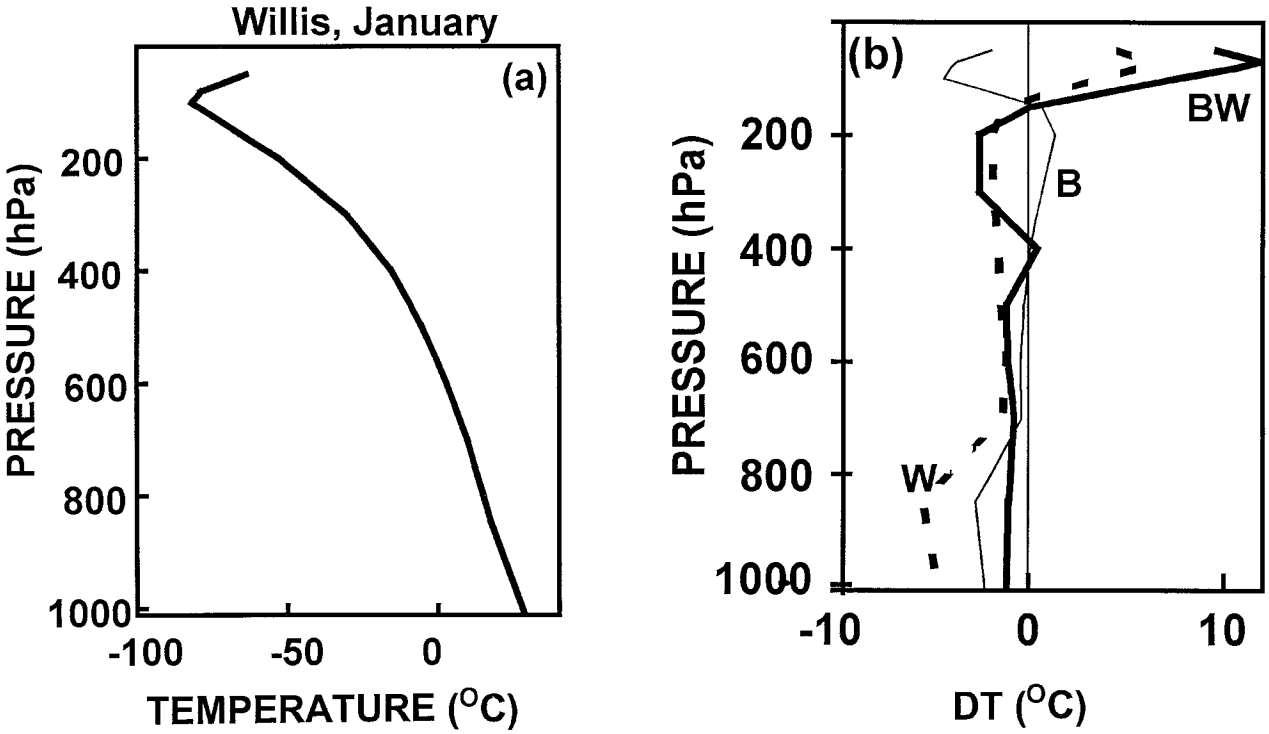

FIG. 8. (a) Mean Willis Island temperature sounding for January (summer) and (b) temperature differences: Willis Island July to January (W), Willis Island January to Barbados August (BW), and Barbados February to August (B). Willis Island data are from Maher and Lee (1977), Barbados data are from C. Landsea (1994, personal communication). Station details are listed in Table 3.

ly dependant on details of the environment and may range between 20 and 35 hPa/°C. This sensitivity to SST is much larger than that in Table 2 from Emanuel (1991), in which the environmental sounding is automatically adjusted to an assumed moist-neutral profile for the defined SST.

We thus emphasize that *this high sensitivity to SST is related to transient changes only and cannot be used for general climatological purposes.* The results are in accord with observations and modelling results (section 4a) and may explain the rapid intensification of polar lows when cold air moves over much warmer water (Rotunno and Emanuel 1987). Two caveats need to be applied.

1) The method assumes instantaneous response to surface changes. While this might reasonably be expected for a cyclone moving over a warm water anomaly and creating enhanced convective activity, ocean cooling may stabilize the lower levels, leading to a gradual decay of the system as a whole.
2) The approach adopted here is to determine the available thermodynamic energy for a system developing from scratch. A preexisting system may respond differently.

Eyewall relative humidity: The sensitivity to surface

TABLE 4. Contributions to the central pressure fall from application of the thermodynamic method to mean soundings at Willis Island in January and Barbados in August (Fig. 8) with eyewall RH of 90%.

Parameter	Willis January	Barbados August
Environmental pressure	1007 hPa	1010 hPa
Pressure following redistribution of existing moist entropy aloft	963	972
Eyewall pressure after air–sea interaction	932 hPa	951 hPa
Final MPI including air–sea interaction and eye development	881 hPa	915 hPa

TABLE 5. Sensitivity of MPI to thermodynamic parameters, utilizing the Willis Island January sounding (Fig. 8a, Table 4) as a basis.

Parameter	Parameter range	MPI (hPa)
SST	27°–31°C	963–832 −33 hPa/°C
Eyewall RH	80%–100%	933–837 −4.8 hPa/%
Environmental pressure	1020–1000 hPa	913–872 2.0 hPa/hPa

RH under the eyewall is around −5 hPa/1% (Table 5), which is substantially lower than that in Emanuel's approach (Table 2). The physical basis is that the higher RH gives an exponential increase of θ_{ES} [Eq. (3)]. This initiates a stronger air–sea interaction cycle, which directly lowers the surface pressure at the eyewall and indirectly enhances the subsidence warming and central pressure deficit. Although observations between surface conditions and intensity in tropical cyclones are almost nonexistent (e.g., Black and Holland 1995), the relatively simple physics and the consistency with different approaches described in section 2 indicate that tropical cyclone intensity will be highly sensitive to surface relative humidity under the eyewall.

For 100% surface humidity and no eye, we obtain a surface pressure of 908 hPa for the January sounding at Willis Island, which is weaker than the central pressure of 883 hPa obtained with a realistic eyewall humidity and an eye. Thus we question the assumption by Emanuel (1986, 1991) that 100% relative humidity can be used either as a proxy for the lack of an eye, or as a worst-case scenario.

Air–sea interaction: There are several aspects of the air–sea interaction cycle that are poorly understood and of concern for this model. These include the potential for surface air to originate inside the eye at substantially lower pressures and higher entropy, and the impact of spray and rain cooling.

Theoretical and observational evidence indicates that spray and rainfall evaporation can have a major impact on the characteristics of the boundary layer in high-wind conditions (Pudov and Petrichenko 1988; Betts and Simpson 1986; Fairall et al. 1995; Black 1993). Recent observations by P. Black (1995, personal communication) indicate that the surface layer in moderate to severe tropical cyclones could contain air that is 4°C cooler than the ocean. This could occur from other processes, such as convective downdrafts, but the observations of Pudov and Petrichenko indicate that substantial temperature reductions can occur in cloud-free conditions. Even for saturated conditions, the reduction of surface θ_E from Black's observations is sufficient to substantially weaken the MPI predicted by the model (e.g., for Willis Island, the MPI weakens from 886 to 934 hPa).

The lower surface pressure in the eye provides a potential source of higher entropy air, which could move outward and enter the eyewall. We can simulate the worst case by adding an eye at each step of the air–sea interaction cycle in Fig. 3 and using the entropy calculated at the cyclone centre. For Willis Island in January, this results in an increased MPI from 883 to 864 hPa. However, the calculated frictional dissipation from Eq. (17) exceeds the buoyant energy in the eyewall and the eyewall equivalent potential temperature reaches an unrealistically high 408 K compared to observations around 380–390 K (section 4).

A plausible, though not entirely convincing, scenario is that the air rising in the eyewall consists of a combination of high entropy air from inside the eye that has moved outward and mixed with drier, lower entropy air spiralling inward above the cold surface layer. Another possibility is that the spray/boundary layer mixing or convective downdraft processes that reduce the surface temperature in the above studies are not effective in the eyewall region. Nevertheless, our understanding is so limited that we simply assume that this process is incorporated in our selected value of surface relative humidity. This is consistent with findings by W. Gray and P. Fitzpatrick (1995, personal communication) that for intense hurricanes the saturated θ_E values in the Shea and Gray (1973) reconnaissance data are equivalent to either surface temperatures of several degrees Celsius less than the SST, or, equivalently, RH of between 80% and 90%.

Environmental pressure: The variation of MPI with environmental pressure has a ratio of around 2 : 1 for the intense cyclones (Table 5). A 1 : 1 relationship is expected from the method of calculating a pressure drop from the environmental value. The higher degree of dependence comes from the inverse relationship between θ_{ES} and P_S [Eq. (3)], which is amplified by warmer T_S. Thus, cyclones in a monsoon trough environment, such as the western Pacific, can be expected to obtain a lower central pressure than those in the North Atlantic trade environment. It is notable that the 12 lowest central pressures on record have occurred in the western North Pacific (Holland 1993).

This central pressure variation does not necessarily indicate a difference of maximum wind speeds, which are related more to the pressure drop from the environment (Atkinson and Holliday 1977). For example, the mean environmental pressures are around 1015 in the North Atlantic and 1005 in the western Pacific, so that the standard Dvorak relationship for cyclone central pressures and maximum winds (Fig. 4) supports the thermodynamic predictions for central pressure but indicates a nearly independent maximum wind.

Vertical eyewall: The sensitivity to the eyewall slope is constrained by our finding (section 3b) that the temperature perturbation above 300 hPa arises almost entirely from moist processes. Thus, eyewall slope in the upper troposphere has little effect. In the lower to mid-troposphere an outward slope of the maximum wind belt is a natural consequence of angular momentum conservation in rising air, which is in thermal wind balance with the warm core structure of the vortex. The maximum vertical motion lies inside the maximum winds and the inner edge of the eyewall cloud generally is more vertical than the sloping maximum wind belt (Jorgensen 1984b). Nevertheless, the eyewall in tropical cyclones slopes outward with height. This slope is sometimes quite marked, with angles as low as 30° from the horizontal (e.g., Jorgensen 1984a,b). But there is strong evidence that intense cyclones have eyewalls that approach vertical and, in many cases, have overhanging

cirrus clouds at high levels (Simpson 1952; Hawkins and Rubsam 1968; Jorgensen 1984a,b).

The maximum sensitivity to the sloping eyewall would be when the inner edge starts at the central pressure, thus enabling a maximum value of surface equivalent potential temperature for the specified environmental parameters. As discussed under air–sea interaction, this produces a maximum 20-hPa change of MPI, combined with an entirely unrealistic cyclone structure and an energy budget that cannot be balanced. Hence, the combination of relatively low sensitivity to eyewall slope in the model and the evidence that very intense cyclones have near vertical eyewalls suggests that our assumption of a vertical eyewall is reasonable.

Moist adiabatic eyewall: The observed temperature profile in eyewalls tends to be greater than moist adiabatic, with an equivalent potential temperature minimum near 700–500 hPa (e.g., Malkus 1958; Hawkins and Rubsam 1968). This is possibly partly due to difficulties with accurately measuring temperature in rain conditions, but other processes such as eyewall entrainment may be important. Many of the observations are also in weaker cyclones that have not reached the MPI for the region and thus may not have fully developed a moist-adiabatic eyewall structure. However, the upper-level values are similar to those near the surface, which may be due to undilute convective cores carrying high entropy air aloft (Malkus 1958) or to additional heating from ice processes (LaSeur and Hawkins 1963). Therefore the moist adiabatic assumption provides a reasonable upper bound on MPI, especially since the upper levels have the biggest impact on the hydrostatic surface pressure calculation.

Eye parameterization: The sensitivity to the parameterization of relative humidity in the eye is small, since the entrainment contributes very little to the eye warming at high levels, where the greatest sensitivity of surface pressure adjustment is found [Eq. (7)]. Allowing pure subsidence increases the degree of eye warming in low levels and requires copious quantities of energy to be sustained, far beyond that available from the ocean surface (section 3d). Markedly increasing the eye relative humidity for the January Willis Island sounding by 30% [limited by a maximum of 80% above 700 hPa, Eq. (9)] means that the model cyclone contains only 75% of the energy available from oceanic interactions. Yet the MPI only changes from 883 to 903 hPa.

The requirements to remain within energetics bounds provides a strong constraint on the eye adjustment that can occur. The actual adjustment is relatively insensitive to the form of the RH structure within these bounds. There is a general decrease of model-derived eye relative humidity as the MPI increases, so that the eye contributes a greater proportion of the pressure fall for more severe cyclones.

Height of warm anomaly: The sensitivity of hydrostatic pressure falls and tropical cyclone intensity to the height of the imposed warming and assumed level of zero pressure perturbation is well known (e.g., Haurwitz 1935). In our method, the additional feedback between surface pressure falls and increases of equivalent potential temperature provide an increased sensitivity, beyond direct hydrostatic calculations. To illustrate this sensitivity, we selectively remove upper levels from consideration in determining the MPI from the January Willis Island sounding. The results (Fig. 9) indicate that reducing the height of the eyewall from 100 to 350 hPa while holding all other parameters constant produces a weakening of 70 hPa in the predicted MPI. We show in section 4c that this is an important factor in the lack of development of tropical cyclones for SST < 26°C and for the weakening of tropical cyclones in extratropical latitudes.

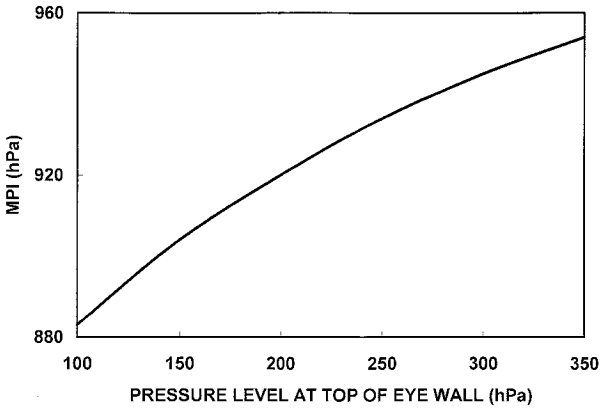

FIG. 9. Variation of MPI for changes in height of the eyewall based on the Willis Island January sounding.

Potential dynamical limitations: The approach adopted here takes no account of additional limitations provided by cyclone dynamics. Some of these limitations are externally imposed, such as adverse environmental vertical shear on cyclone development (Merrill 1993). W. Gray (1983, 1995, 1996, personal communications) also has indicated that a potential limitation arises from the manner in which frictional dissipation of the azimuthal flow rises much faster than the increase of buoyant energy needed to maintain the required secondary circulation. The energy budget in this study [Eqs. (15)–(17)] indicates that the thermodynamic limitation is reached before this dynamical limit. However, this highly simplified budget may not be fully representative of real cyclones. In any case, such dynamical limits can only produce a limitation on cyclone intensity that is stronger than the purely thermodynamic approach used here. Thus our assumption of the MPI as an absolute limitation on tropical cyclone intensity remains valid.

Potential for ''hypercanes'': The Carnot-model approach derived by Emanuel (1991) contains an instability in which beyond a certain ocean or outflow temperature the thermodynamics no longer converge and a runaway intensification occurs. Emanuel called this the

''hypercane'' region of the phase space (see his Fig. 2). The same instability occurs here, but it requires very extreme conditions to develop. For example, changing the Willis Island SST to 40°C, while holding the remainder of the sounding constant, provides an eyewall surface pressure of 815 hPa and central pressure of 622 hPa. Increasing the SST further to 42°C results in a breakdown of the solution procedure.

Observations of temperature profiles over oceans of greater than 30°C surface temperature do not exist. However, the above extreme example could not be achieved in physically realistic situations, as the deep atmospheric sounding would be in convective–radiative adjustment with this surface condition. Hypothetical situations, such as the asteroid impact examined by Emanuel et al. (1995), are moot and beyond the scope of this study.

4. Comparison with observations of MPI

a. Case study applications

Tropical Cyclone Kerry (1979): Black and Holland (1994) present a detailed analysis of the boundary layer of Tropical Cyclone Kerry over the Coral Sea northeast of Australia. The cyclone was near its peak intensity and had caused significant ocean surface cooling by mixing and upwelling. While Kerry was also affected by dynamical processes in the form of a strong vertical shear, the detail of the boundary layer provides a rare example for direct application of thermodynamical models. The observed maximum intensity of 955 hPa was much weaker than the climatological value of 886 hPa obtained from the February mean Willis Island sounding. This concurs with the findings by Merrill (1988), Evans (1993), and DeMaria and Kaplan (1994) that very few tropical cyclones reach the climatological MPI. However, when the observed ocean cooling of 2°C (T_S = 26°C) and P_{env} = 1003 are used, the derived MPI changes to 958 hPa, which is close to the observed value.

Supertyphoon Flo (1990): Flo occurred during the TCM-90 field experiment in the western North Pacific (Elsberry et al. 1990), with an estimated maximum intensity from the Joint Typhoon Warning Center of 75 m s^{-1} [881 hPa from Eq. (13)] that is near to the maximum for the region. National Aeronautics and Space Administration (NASA) DC-8 reconnaissance flights on two consecutive days while Flo was developing to supertyphoon stage provided the first direct upper-tropospheric observations of a severe cyclone in 30 years, together with a dropsonde in the inner eyewall and eye region, and an observation of 891 hPa surface pressure. Merrill and Velden (1996) utilized the excellent data obtained during TCM-90 and postanalyses by the National Meteorological Center (now the National Centers for Environmental Prediction) to produce the first detailed three-dimensional analysis of a tropical cyclone outflow layer. They show that the potential temperature of the upper outflow level increases as the cyclone intensifies, in support of our model results.

The NASA DC-8 flew two sorties into the storm at approximately 0600 UTC on 16 and 17 September at an altitude of 190–200 hPa. Radial profiles of observed air temperature and winds for a butterfly pattern flown on 17 September are shown in Fig. 10a. The eye at this stage was shrinking rapidly as the cyclone neared maximum intensity (Elsberry et al. 1990, 96), and estimates from satellite imagery indicate a radius of less than 20 km or around 10 km inside the RMW. Calculated θ_E profiles based on assumed saturation in the eyewall region and dry air in the eye (Fig. 10b) clearly indicate a sharp increase toward the inner eyewall. The entropy increase is also largely constrained to inside the radius of maximum winds, but this did not occur in Hurricane Cleo (LaSeur and Hawkins 1963) and Hurricane Hilda (Hawkins and Rubsam 1968).

We constructed an environmental sounding from a composite of available soundings within 1000 km of Flo and matched above 350 hPa to the 800-km radius analysis in Fig. 4a of Merrill and Velden (1996). We also used observed values of P_{env} = 1010 hPa and SST = 29.9°C. Our model predictions indicate that the analysed maximum intensity of the typhoon (Table 6) was close to the potential intensity for the environment in which the typhoon was embedded.

The maximum θ_E observed on each of the DC-8 flights was 374 and 381 K. These are consistent with the maximum outflow potential temperature found by Merrill and Velden (1996). The MPI for the constructed environmental sounding was 890 hPa, with a surface θ_E = 382 K (Table 6), which concurs with the observations. Inserting the observed θ_E values at the ocean surface under the inner eyewall in the model produced excellent agreement with the analyzed and observed intensities (Table 6). In addition to confirming the model parameterizations and assumptions, this indicates that there is potential for estimation of tropical cyclone intensity (central pressure) from upper-tropospheric observations of equivalent potential temperature.

Numerical model results: Bender et al. (1993) reported a numerical modeling study of the sensitivity to oceanic changes associated with hurricane ocean interactions, which do not contain other adverse environmental effects. We compare their results with the thermodynamic estimates of MPI by the following method. Their environmental temperature profile was used together with an assumed environmental pressure of 1010 hPa, and the eyewall relative humidity was adjusted to match surface equivalent potential temperatures (their Plate 1). The results (Table 7) provide a good approximation to the full numerical model predictions.

We conclude that our approach can reproduce observed and maximum intensities, and specific thermodynamic features, at least for this limited set of exam-

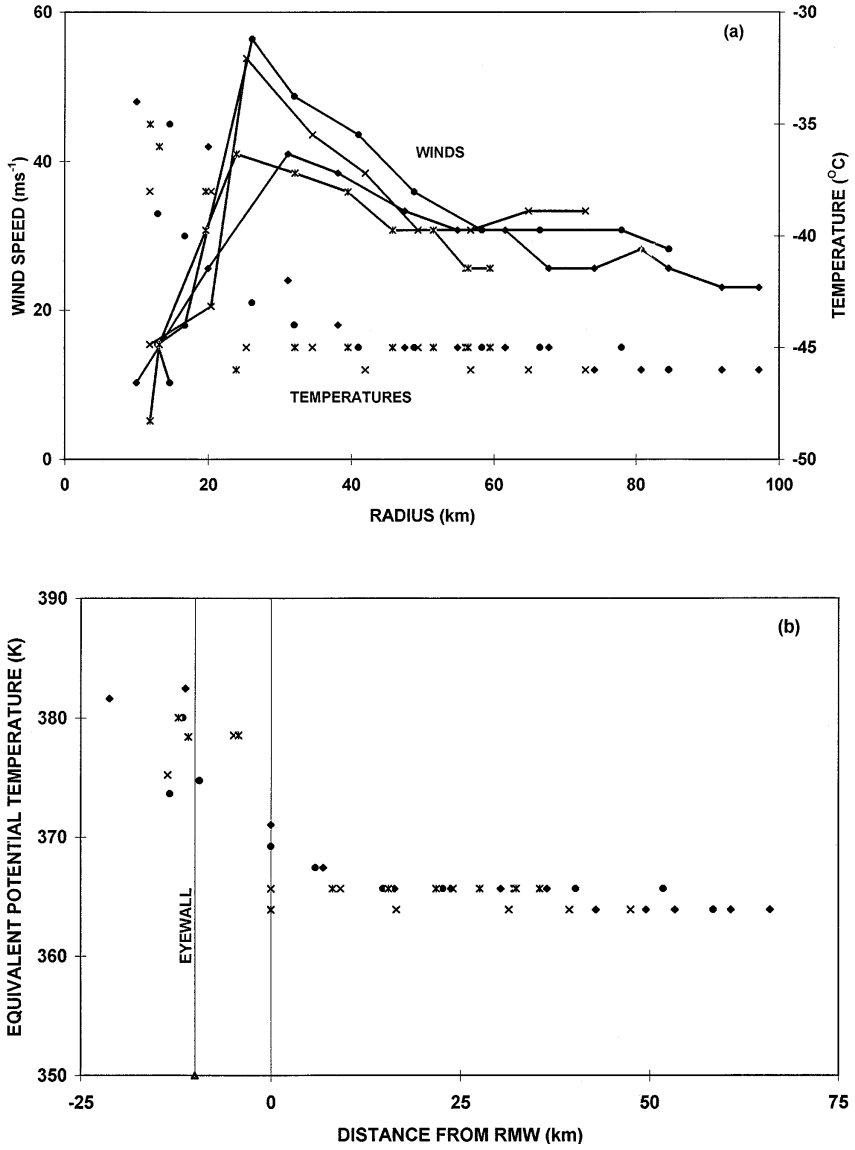

FIG. 10. Radial profiles at the 190–100-hPa level of (a) wind speed and temperature, and (b) equivalent potential temperature obtained from a NASA DC-8 reconnaissance of Supertyphoon Flo. The abscissa in (b) is relative to the RMW for each flight leg and the approximate position of the inner eyewall is shown.

TABLE 6. Comparison of analyzed central pressures with model predictions for Supertyphoon Flo (1990) based on NASA DC-8 observations of θ_E in the first two lines and the maximum intensity in the bottom line.

Date	θ_{Emax} (K)	Analyzed P_C (hPa)	Model P_C (hPa)
16 Jun	374 (obs)	921	913
17 Jun	382 (obs)	891	883
Maximum intensity	380 (pred)	885	890

ples. Further analysis is being undertaken to determine the general applicability.

b. The Dvorak pattern recognition technique

One of the interesting aspects of tropical cyclones is the remarkably robust method for estimating the intensity from satellite imagery developed by Dvorak (1975, 1984). While this method has significant errors, it implies that the generic aspects of the intensity can be

TABLE 7. Comparison of thermodynamic model predictions of MPI with the numerical modeling experiments for a cyclone in a 5 m s^{-1} basic flow by Bender et al. (1993). The numerical model results from Bender et al. are indicated in parentheses.

	T_S at center (°C)	Eyewall RH	Eyewall θ_{ES} (K)	MPI (hPa)
No ocean coupling	28.8	0.76	362 (>355)	944 (940)
Ocean coupling	27.3	0.81	357 (>350)	962 (956)

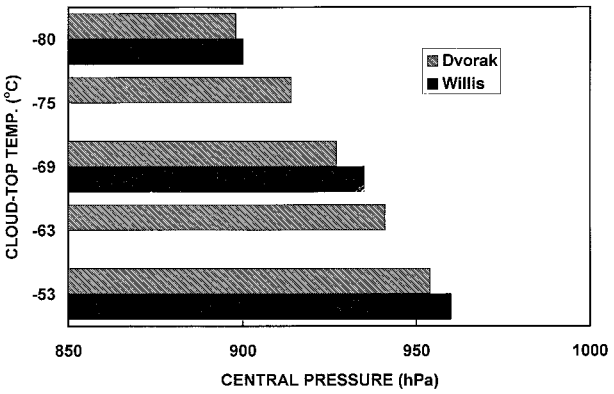

FIG. 11. Comparison of variation of central pressure with cloud-top temperature in the Dvorak technique and equivalent detrainment levels for Willis Island.

determined by only a knowledge of the cloud distribution in the core region. As discussed by Merrill (1993), the most intense cyclones have a characteristic pattern of an eye embedded in a ring or band of high cloud. The cyclone intensity is then directly related to a range of parameters, including the cloud-top temperature in the eyewall.

We compared the model presented here with the Dvorak eyewall cloud-top temperatures by the following method. The ''Eye Pattern'' box on Dvorak's check sheet (e.g., box 2c on p. 2.16 of Merrill 1993) was used to determine the ''E-number'' based on cloud-top temperatures. This was modified by an eye adjustment of 0.5 to relate nearly to the Willis Island January MPI. The monthly Willis Island sounding with a cloud detrainment temperature most closely matching the Dvorak cloud-top temperatures was then used to derive an equivalent intensity. The results in Fig. 11 indicate good agreement between our thermodynamic technique and the Dvorak approach, and emphasize that the maximum height of the warm core and vigor of the convection is a major factor for determining cyclone intensity. Further refinements of the Dvorak technique to account for observed environmental profiles could be derived by a combination of the two approaches.

c. Empirical relationships with SST

Several empirical estimates of the relationship between MPI and SST have been developed (Merrill 1988; Evans 1993; DeMaria and Kaplan 1994) by matching historical records of tropical cyclone intensity with monthly mean SST. The most intense cyclone found for each SST is assumed to be close to the MPI. All of these relationships have the approximate form of that derived for the North Atlantic by DeMaria and Kaplan shown in Fig. 12a.[2] The curve indicates a steady, linear increase of MPI (decreasing central pressure) for SST between 20° and 26°C, followed by a sharp rise from 26° to 28°C, then an apparent approach to a limiting value beyond 29°C.

Figure 12a also contains a scatter of MPIs derived by utilizing monthly mean soundings and surface pressures for the whole year at the stations listed in Table 3. We used the observed mean surface temperature for the small, exposed coral cay of Willis Island. The other stations were obviously affected by land or elevation effects at the surface, so the surface temperature was set at 1°C less that the monthly mean SST off the coast [derived from the COADS (Comprehensive Ocean–Atmosphere Data Set database] and the remainder of the sounding was assumed to be in equilibrium with the oceanic environment. The resulting MPIs indicate that the empirical curve comprises two separate families of decaying and developing tropical cyclones.

We consider that the lack of agreement between the thermodynamic and empirical estimates of MPI for SST < 26°C in Fig. 12a is due to cyclones that develop at higher SST gradually decaying as they move over colder waters. DeMaria and Kaplan's empirical curve in this region indicates an almost constant slope of 2.5 hPa $°C^{-1}$, which is substantially less than the 15–35 hPa $°C^{-1}$ found by the sensitivity analysis for SST changes with a fixed environment (Table 5). This suggests that other processes are operating, such as the ocean surface decoupling discussed in section 3f, movement into a rapidly changing environment, or the inertial stability processes described by Weatherford and Gray (1988). The empirical curves for this SST range vary widely across ocean basins (Evans 1993) indicating that a range of decay mechanisms occur.

The developing cyclone set in Fig. 12b is the focus of this study. For SST < 26°C our method indicates that there is insufficient available thermodynamic energy for tropical cyclone development. There is some scatter of MPIs near SST = 25°–26°C, which may be real or may arise from our somewhat arbitrary selection criteria for development of an eye. As the SST increases beyond 26°C the scatter in predicted MPIs from different ocean basins is small and close to the empirical curve. A rapid increase in MPI of approximately 30 hPa $°C^{-1}$

[2] We used the Dvorak (1984) North Atlantic relationship (Fig. 4) to convert from DeMaria and Kaplan's maximum wind values.

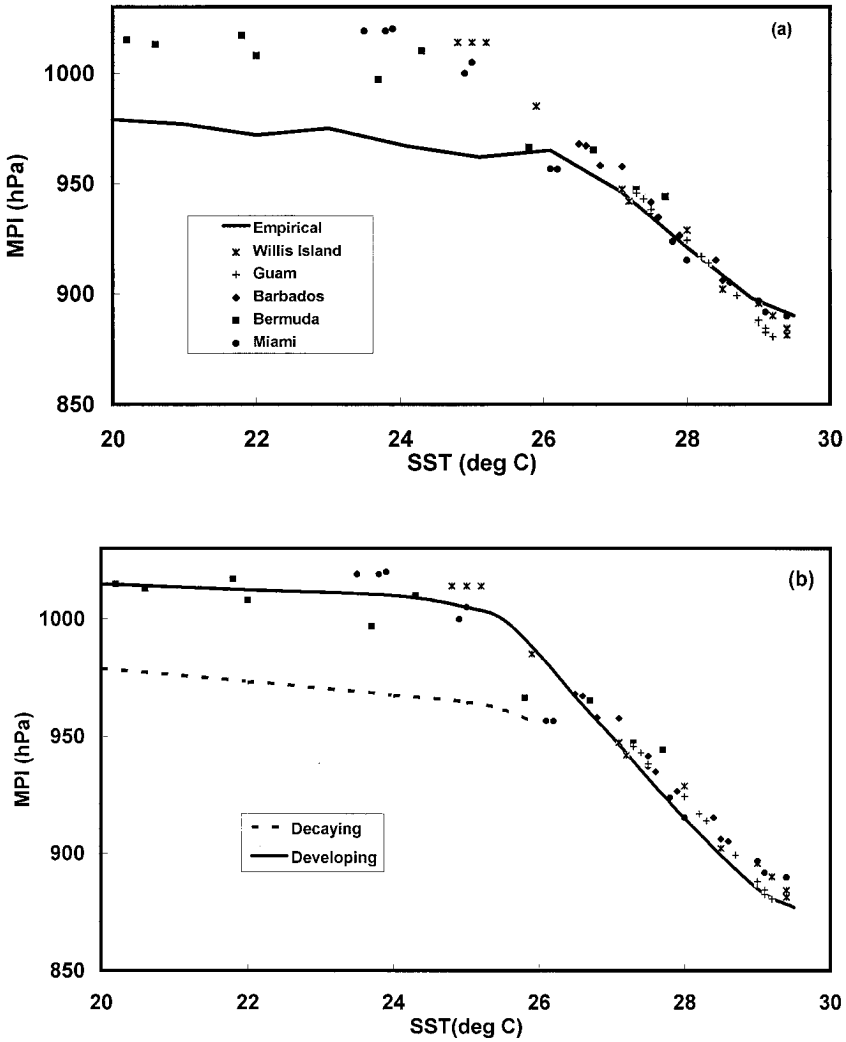

FIG. 12. Scatterplots of the SST variation of MPI estimates from the indicated stations: (a) imposed upon the empirical curve for the North Atlantic derived by DeMaria and Kaplan (1994) and (b) new curves indicating the differences between developing cyclones and those that are decaying while moving over colder water.

is found for 26°C < SST < 29°C. Only limited tropical cyclone data are available for SST > 29°C in the North Atlantic, and the flattening of the MPI curve in Fig. 12a is in part due to inadequate sampling (DeMaria and Kaplan 1994). However, since the rate of increase of predicted MPIs also decreases at higher SST (Fig. 12b) and similar profiles are obtained in other ocean basins (Evans 1993), we suggest that there may be a real limitation.

We emphasize that the SST increase has a secondary role in determining tropical cyclone intensity, which is to establish the ambient conditions for cyclone development and intensification *prior* to the cyclone development. The rapid increase in MPI as the SST warms from 26° to 29°C arises from the concomitant increase in capacity to develop a warm core above 300 hPa (Fig. 13). Soundings over ocean temperatures colder than 26°C can support only a weak warming that is generally constrained to below 250–300 hPa and is insufficient for cyclone development (e.g., Fig. 9). This explains the well-known requirement for a minimal SST of 26.5°C for cyclone development (e.g., Palmen 1948; Gray 1968) and we concur with Emanuel (1986) in this assessment. All of the MPIs of less than 900 hPa arose from soundings that enabled the eyewall warming to be a maximum at 150–200 hPa.

This capacity for developing an upper warm core arises from a combination of changes in *both* the tropopause and the lower troposphere, as is indicated by the changes of monthly mean soundings at Willis Island and Miami in Fig. 14. At Willis Island (Fig. 14a), the transition to a tropical cyclone season occurs by a combination of

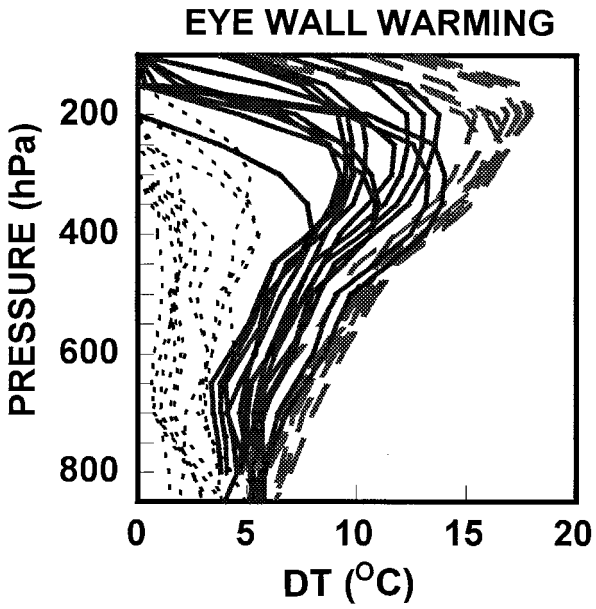

FIG. 13. Eyewall warming after the air–sea interaction cycle derived from monthly mean soundings at Willis Island, Guam, and Bermuda. Short dash lines indicate soundings that failed to develop a cyclone, and large dashed lines indicate soundings for which MPI $<$ 900 hPa.

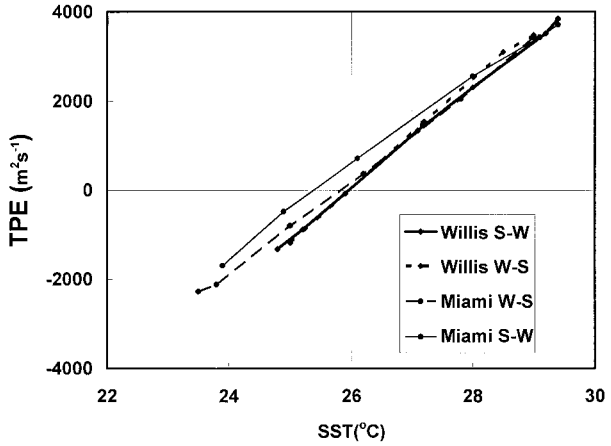

FIG. 15. Potential energy for cyclone development integrated from the surface to 100 hPa for the profiles in Fig. 14 (W–S indicates winter to summer transition and vice versa).

warming below 700 hPa and cooling of the tropopause but with essentially no changes to the midlevel temperatures. Thus it is expected that a rapid increase of MPI should occur. As the ocean temperatures increase further, the entire sounding warms up at approximately the same rate. This supports our suggestion that the MPI increases rapidly with SST between 26° and 29°C, then increases less rapidly at higher temperatures. Miami,

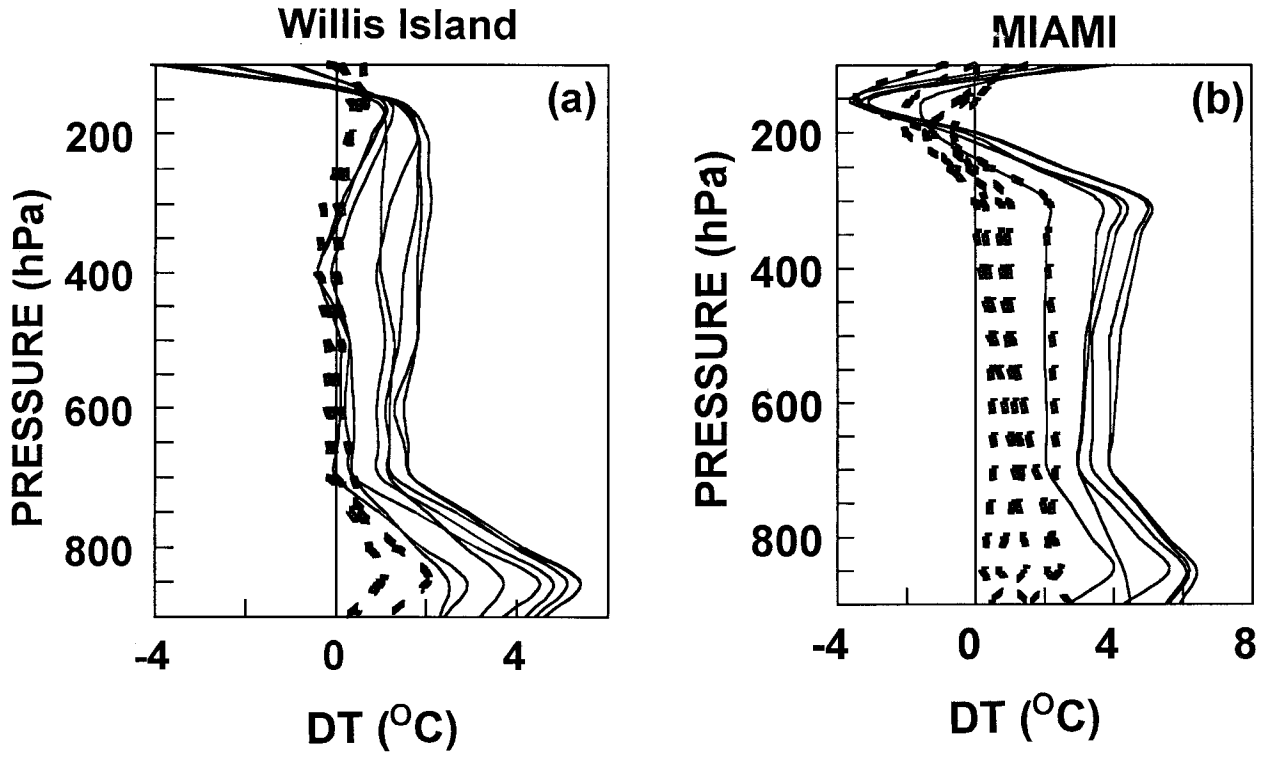

FIG. 14. Variations of monthly mean soundings from the month of coldest SST at (a) Willis Island and (b) Miami. Dashed lines indicate months where the MPI was below tropical cyclone strength.

which is effected by midlatitude systems in winter, initially warms throughout the troposphere up to about 300 hPa and cools at the tropopause (Fig. 14b). The transition to the tropical cyclone season is accompanied by the same enhanced low-level warming and tropopause cooling observed at Willis Island.

Calculations of TPE [Eq. (14)] between the surface and 100 hPa for Willis Island and Miami (Fig. 15) provide a remarkably linear transition from negative to positive values at SST of 26°C. This transition displays no hysteresis when going from winter to summer and returning to winter. We suggest that global maps of this parameter might provide a more accurate delineation of regions capable of developing tropical cyclones than using SST alone.

Preliminary investigations indicate that the lower-troposphere warming arises from a combination of radiation trapping by water vapor, warm rain processes, and horizontal advection. This aspect has not been reported previously and is as important to the provision of potential energy for cyclone intensification as is the lifting of the tropopause. It also supports the well-known tendency for tropical convection to become ubiquitous and vigorous for SST $>$ 26°C, which Emanuel (1986) has related to the capacity for convective instability in the atmosphere.

d. Implications for climate change

The implications for climate change are fully developed in a study to be reported separately. The important feature is that the increases of SST arising from anthropogenic climate change is associated with a substantial warming of the upper atmosphere throughout the Tropics. The result is that the SST relationship in Fig. 12 cannot be extrapolated to the climate change SSTs. Rather, the entire curve moves to higher SST, with a new cyclogenesis cut off near 27°–28°C and modest increases of MPI at the extreme end. This concurs with the observations by Landsea and Gray (1994) and the conclusions by Lighthill et al. (1994).

5. Conclusions

The thermodynamic limitations on the maximum potential intensity (MPI) of tropical cyclones have been examined by a review of previous work (Table 1) and development of the new approach outlined in Figs. 2 and 3.

Pioneering work by Byers (1944) and Riehl (1948, 1954) has shown that there is insufficient available thermodynamic energy in the atmosphere to generate intense tropical cyclones. They suggested that the increase of moist entropy when surface pressure decreases over an ocean of constant surface temperature could provide the required source of additional energy. Malkus and Riehl (1960) noted that redistribution of surface moist entropy aloft could lead to significant pressure falls underneath the eyewall, but they did not include the eye region in their analysis. Miller (1958) developed a relationship between eye warming by subsidence and MPI but neglected the important oceanic feedback.

Kleinschmidt [1951; see Gray (1994) for a translation] postulated the tropical cyclone as a Carnot heat engine, in which the heating occurs at the ocean surface and the cooling occurs by radiation in the cold outflow layer. A series of papers summarized in Emanuel (1991) extended those of Malkus and Riehl and Kleinschmidt. The available energy for work is determined by the maximum entropy difference between the cyclone center and environment. This analysis has substantially extended our knowledge of tropical cyclone thermodynamics; however, the basic approach is extremely sensitive to the arbitrary choice of surface relative humidity in the environment (which is used to derive an environmental sounding) and of 100% relative humidity in a cloud filled cyclone center (Table 2). A problem also arises with the specification of the outflow, which is assumed to be symmetric and occurring under conditions indicative of the mean environment in the near vicinity of the storm center. In real cyclones this outflow is highly asymmetric, constrained to a narrow layer, and normally directed into the deep tropics or to subtropical latitudes. We note that the maximum intensity in this approach also is defined by a vertical saturated moist adiabat at the cyclone center. If we neglect the small energy contributed to developing an anticyclonic circulation in Emanuel's approach [the second term in the exponent of Eq. (2)], and assume that the outflow temperature is equivalent to the height of the warm anomaly that is developed, then the fundamental thermodynamics become quite similar to the eyewall derivation adopted here.

The model presented here adopts a more traditional thermodynamic approach (Table 1, Figs. 2 and 3). The eyewall and eye region of the cyclone are explicitly included, together with the moist entropy gain from feedback between a developing cyclone and the warm ocean. We are only interested in the properties of surface air at the eyewall; its origin and trajectory are not required. Boundary conditions are provided by the environmental surface pressure, an atmospheric temperature sounding and ocean temperature.

Surface moist entropy is redistributed aloft in the eyewall, which is assumed to be vertical and have no entrainment. A simple parameterization of an eye utilizes an assumed constant moist entropy at the level of that obtained under the eyewall at the surface and a vertical profile of relative humidity that is dependent on the cyclone intensity. This parameterization is further constrained by a simple energy budget and is assumed to provide the end result of subsidence and eyewall entrainment. The resulting warming of the atmospheric column over the center results in calculated surface pressure falls from hydrostatic balance. The method iteratively converges to a stable estimate of MPI for all

known conditions that are representative of the earth's atmosphere.

A detailed analysis indicates that the major sensitivity is to the relative humidity of surface air under the eyewall, the height of the warm anomaly that is developed, and transient changes of ocean temperature, which concurs with previous studies (Malkus and Riehl 1960; Emanuel 1991). These are considered to be real sensitivities that govern much of the intensity variability of tropical cyclones. The depth of warming and adjustment to changing SST are deterministic. A significant assumption has to be made on a representative value of surface RH under the eyewall. This region has not been adequately sampled by direct observations and could be markedly affected by spray and rainfall. In addition the near surface air passes under the eyewall and into the eye (Marks et al. 1992), where it will gain substantially higher moist entropy. Some of this air moves out into the eyewall, where it is mixed with above surface air in unknown proportions. In the absence of better information, we use a standard RH of 90% and surface temperature of 1°C less than the SST to define the moist entropy of the air rising into the eyewall. This lies on the conservative end of published estimates

Excellent agreement is found from application of the method to observations, including case studies of Hurricane Hilda (Hawkins and Rubsam 1968), Tropical Cyclone Kerry (Black and Holland 1995), and Supertyphoon Flo (1990); the Dvorak (1984) pattern recognition relationships; and the empirical values of MPI related to monthly mean conditions (DeMaria and Kaplan 1995). We suggest that these empirical values are composed of two distinct families of tropical cyclones: those that are decaying while moving over colder waters and those that are developing.

We find generally insufficient thermodynamic energy available for cyclone development at SST < 26°C (Fig. 12b). Some scatter between 24° and 26°C may be related to our arbitrary cut-off for developing an eye but also could be real. In particular, it is possible that local advective or other processes could result in an atmosphere sufficient to support cyclone development even though the ocean temperature is less than 26°C. At the transition from cold to warmer oceans near SST = 26°C the atmosphere rapidly warms in the lower troposphere and develops a colder, higher tropopause, while the midlevels remain essentially unchanged (Fig. 14). This provides a markedly increased potential for warming from moist convection, especially in the upper troposphere, and enables sufficient initial surface pressure falls for the air–sea interaction cycle required to extract additional oceanic energy to commence. This lower-warming, upper-cooling develops further as the SSTs increase from 26° to 28°C and, when combined with the increasing efficiency of air–sea interaction leads to a very rapid increase of MPI of about 30 hPa °C^{-1}. At higher SSTs, the middle atmosphere also begins to warm and the tropopause becomes capped at around 100 hPa, resulting in a decreased MPI tendency. A stronger cap is placed on maximum winds, since these vary approximately as the square root of the pressure drop from the environment (Holland 1980; Atkinson and Holliday 1977)

We have insufficient atmospheric information for direct thermodynamic estimates of MPI for SSTs above 29.5°C, but both the evidence for atmospheric stabilisation and empirical data (Evans 1993) indicate that there may be an MPI cap near SST = 30°C. We strongly caution against forcing an exponentially increasing trend of MPIs for higher SSTs.

The relative contributions of warming by moist processes in the eyewall and by the combination of dry subsidence and mixing in the eye are of some interest. We find that the upper-troposphere warming above 250 hPa is almost entirely due to moist ascent in the eyewall (Fig. 6). Since the moist and dry adiabats are essentially the same at high altitude, dry subsidence in the eye introduces no additional warming. It is this feature that allows us to neglect the slope of the eyewall in estimating the MPI.

The additional warming in the eye becomes important below 300 hPa. Combining the eyewall and eye processes produces the characteristic maximum temperature anomaly near 300 hPa. The additional eye warming is essential to the overall cyclone structure and, in particular, to the sharp pressure gradients required to maintain the very high winds that are observed near the surface. But this only accounts for about 20%–40% of the total pressure fall. It is the capacity for ascent to high levels in the eyewall, and the associated upper-tropospheric warming, that enables development of very severe tropical cyclones.

We combine these results with previous observational and theoretical work to speculate on the potential processes operating to bring a severe tropical cyclone to its maximum intensity.[3] Initially a region of moist convection establishes a broad area of warming, especially in the upper troposphere, and lowering of surface pressures. If the vertical windshear is too large, this low-pressure region cannot develop. Substantial mesoscale activity occurs in this region and is ultimately responsible for the seedling that becomes the tropical cyclone. Once an eye has formed, the contraction cycle discussed by Shapiro and Willoughby (1982) and Willoughby et al. (1982) enhances and focuses the pressure falls. The convective disequilibrium for this eyewall–eye circulation is provided largely by the air–sea interaction process. As the air–sea interaction converges by the processes described in Fig. 5, the eyewall contraction ceases and maximum intensity is achieved. Should a secondary eyewall develop, the eye will collapse and the surface pressure will drop to the broader level sustainable by

[3] I am indebted to Hugh Willoughby for discussions that helped clarify this conclusion.

the upper-level temperature anomaly developed by moist processes. A new eyewall cycle will again focus the lower warming and bring about reintensification.

These results are applicable to environments in which the atmosphere is in a convective–radiative equilibrium with the ocean surface. If a cyclone and its air mass move over a local warm pool of water, then more vigorous moist convection and rapid adjustment to the higher MPI could be expected. As discussed by Rotunno and Emanuel (1987), this mechanism may be of significance to the development of polar lows and other marine systems, which are observed to develop rapidly as cold air moves over warmer water; in this case, the large amount of energy available from the surface overcomes the requirement for a warm core at high levels. Developing cyclones moving over or creating cold surface water in the core region also could be expected to have their intensification rapidly terminated. However, fully developed systems that move over colder water may decouple from the surface and decay gradually, since the upper warm core is capable of maintaining a substantial surface pressure fall (unless there are destructive processes, such as strong vertical windshear operating). This provides an explanation of the gradual, linear decay of MPI for SST < 26°C found in empirical studies (e.g., Fig. 12a). We note, however, that this curve varies considerably from ocean basin to ocean basin (Evans 1993), implying that substantially different decay mechanisms are operating.

While the general agreement with observations is encouraging, considerable uncertainty remains. Inherent assumptions of a vertical eyewall with constant saturated moist entropy, the eye paramaterization, and the lack of direct dynamical effects have been discussed in detail. We show that these assumptions result in MPI estimates that are inherently conservative and to the extreme side of possible results. Further, the sensitivity to relative humidity of the eyewall and to ocean cooling has not been adequately investigated. For example, spray and rainfall in the high wind region could have major impact on the realizable MPI of some systems. The maximum wind speed achievable with a given pressure fall also needs further consideration. Here the maximum is ultimately limited by dissipation of kinetic energy at the ocean surface, which increases as the square of the wind but also is a function of the inflow trajectory (Malkus and Riehl 1960). Empirical relationships relating pressure drop and maximum wind speed directly therefore may be oversimplified, as can be seen by the observed scatter (e.g., Neal and Holland 1976) and the inherently different relationships in the North Atlantic and western North Pacific (Fig. 4). Further, we suggest that empirical relationships between environmental parameters, such as vertical wind shear, establishment of outflow jets, etc. (e.g., Merrill 1993), need to be revised to accommodate the strong thermodynamic inhibitions on cyclone intensity described in this study.

The method is straightforward to apply, requiring only a sounding and surface pressure and temperature, and is applicable to daily estimates of MPI based on operational numerical model fields. We will be reporting separately on application of the method in forecasting and to global climate models to provide an objective estimates of the potential changes in tropical cyclone activity resulting from climate change.

Acknowledgments. This study benefited considerably from discussions with Chris Landsea, Ann Henderson-Sellers, Kendal McGuffie, Pete Black, Hugh Willoughby, and Frank Marks, and from review comments provided by Pat Fitzpatrick, Bill Gray, Mark DeMaria, and Kerry Emanuel. Chris Landsea also provided some of the sounding and SST data that were used. This study forms part of the Tropical Cyclone Coastal Impacts Program and has been partially supported by the by the Australian National Greenhouse Advisory Committee, Department of the Environment, Sport and Territories and the U.S. Office of Naval Research under Grants N-00014-94-I-0556 and N-00024-94-1-0493.

APPENDIX

Definition of Terms

Subscripts and superscripts:

X_c	Value at the cyclone center
X_{env}	Environmental value
X_{eye}	Eye value
$X_{eyewall}$	Eyewall value
X_{madiab}	Moist adiabatic value
X_{max}	Maximum value
X_S	Surface value
X^*	Saturated value
Δ	Difference or change in a parameter
c_p	Specific heat of dry air
f	Coriolis parameter
$\mathbf{F}$	Friction
g	Gravitational acceleration at sea level
$\mathbf{l}$	Unit vector along streamline
L_v	Latent heat of vaporization
M	Mixing ratio of saturated eyewall air into the eye
MPI	Maximum potential intensity
p, P	Pressure
P_T	Pressure at the level of no temperature perturbation
q	Water vapor mixing ratio
r	Radius form the cyclone center
r_{env}	Size of the cyclone, taken as radius of outer closed isobar or gale force winds
RMW	Radius of maximum winds
R_d	Gas constant for dry air
RH	Relative humidity
S	Entropy
T	Temperature
T_{adiab}	Temperature following an adiabatic lapse rate

T_L	Temperature of the lifting condensation level
T_{out}	Outflow temperature
T_v	Virtual temperature
v	Wind speed
ϵ	Thermodynamic efficiency of the Carnot cycle
θ	Potential temperature
θ_{T}	Potential temperature at cloud top
θ_E	Equivalent potential temperature
θ^*_{EC}	Saturated equivalent potential temperature in the eyewall
$\theta_{E,\text{Eye}}$	Constant equivalent potential temperature throughout the eye

REFERENCES

Atkinson, G. D., and C. R. Holliday, 1977: Tropical cyclone minimum sea level pressure maximum sustained wind relationship for the western North Pacific. *Mon. Wea. Rev.,* **105,** 421–427.

Bender, M. A., I. Ginis, and Y. Kurihara, 1993: Numerical simulations of tropical cyclone–ocean interaction with a high-resolution coupled model. *J. Geophys., Res.,* **98,** 23 245–23 263.

Betts, A. K., and J. S. Simpson, 1987: Thermodynamic budget diagrams for the hurricane subcloud layer. *J. Atmos. Sci.,* **44,** 842–849.

Black, P. G., and G. J. Holland, 1995: The boundary layer of Tropical Cyclone Kerry (1979). *Mon. Wea. Rev.,* **123,** 2007–2028.

Black, R. A., H. B. Bluestein, and M. L. Black, 1994: Unusually strong vertical motions in a Caribbean hurricane. *Mon. Wea. Rev.,* **122,** 2722–2739.

Bolton, D., 1980: The computation of equivalent potential temperature. *Mon. Wea. Rev.,* **108,** 1046–1053.

Byers, H. R., 1944: *General Meteorology.* McGraw-Hill, 645 pp.

DeMaria, M., and J. Kaplan, 1994: Sea surface temperature and the maximum intensity of Atlantic tropical cyclones. *J. Climate,* **7,** 1324–1334.

Dvorak, V. F., 1975: Tropical cyclone intensity analysis and forecasting from satellite imagery. *Mon. Wea. Rev.,* **103,** 420–430.

——, 1984: Tropical cyclone intensity analysis using satellite data. NOAA Tech. Rep. NESDIS 11, 47 pp. [Available from NOAA–NESDIS, World Weather Building, Washington, DC 20235.]

Ebert, E. E., and G. J. Holland, 1992: Observations of record deep convection in Tropical Cyclone Hilda. *Mon. Wea. Rev.,* **120,** 2240–2251.

Elsberry, R. L., B. C. Deihl, J. C.-L. Chan, P. A. Harr, G. J. Holland, M. Lander, T. Neta, and D. Thom, 1990: ONR tropical cyclone motion initiative: Field experiment summary. Tech. Rep. NPS-MR-91-001, 106 pp. [Available from Naval Postgraduate School, Monterey, CA 93943-5000.]

Emanuel, K. A., 1986: An air–sea interaction theory for tropical cyclones. Part 1: Steady-state maintenance. *J. Atmos. Sci.,* **43,** 585–604.

——, 1987: The dependence of hurricane intensity on climate. *Nature,* **326,** 483–485.

——, 1991: The theory of hurricanes. *Annu. Rev. Fluid Mech.,* **23,** 179–196.

——, K. Speer, R. Rotunno, R. Srivastava, and M. Molina, 1995: Hypercanes: A possible link in the global extinction scenarios. *J. Geophys. Res.,* **100,** 13 755–13 765.

Evans, J. L., 1993: Sensitivity of tropical cyclone intensity to sea surface temperature. *J. Climate,* **6,** 1133–1140.

Fairall, C. W., J. D. Kepert, and G. J. Holland, 1995: The effect of sea spray on surface energy transports over the ocean. *Atmosphere Ocean System,* **2,** 121–142.

Frank, W. M., 1984: A composite analysis of the core of a mature hurricane. *Mon. Wea. Rev.,* **112,** 2401–2420.

Gentry, R. C., T. T. Fujita, and R. C. Sheets, 1970: Aircraft, spacecraft, satellite and radar observations of Hurricane Gladys, 1968. *J. Appl. Meteor.,* **9,** 837–850.

Gray, S. L., 1994: Theory of mature tropical cyclones: A comparison between Kleinschmidt (1951) and Emanuel (1986). JCMM Rep. 40, 50 pp. [Available from Joint Centre for Mesoscale Meteorology, University of Reading, P.O. Box 240, Reading, Berkshire RG6 2FN, United Kingdom.]

Gray, W. M., 1968: Global view of the origin of tropical disturbances and storms. *Mon. Wea. Rev.,* **96,** 669–700.

Haurwitz, B., 1935: The height of tropical cyclones and the ''eye'' of the storm. *Mon. Wea. Rev.,* **63,** 45–49.

Hawkins, H. F., and D. T. Rubsam, 1968: Hurricane Hilda, 1964. 2. Structure and budgets of the hurricane on October 1, 1964. *Mon. Wea. Rev.,* **96,** 617–636.

Hirschberg, P. A., and J. M. Fritsch, 1993: On understanding height tendency. *Mon. Wea. Rev.,* **121,** 2646–2661.

Holland, G. J., 1980: An analytic model of the wind and pressure profiles in hurricanes. *Mon. Wea. Rev.,* **108,** 1212–1218.

——, 1993: Ready reckoner. *Global Guide to Tropical Cyclone Forecasting* WMO/TD-560, G. J. Holland, Ed., World Meteorological Organization, 9.1–9.26.

——, T. D. Keenan, and G. D. Crane, 1984: Observations of a phenomenal temperature perturbation in Tropical Cyclone ''Kerry'' (1979). *Mon. Wea. Rev.,* **112,** 1074–1082.

Jorgensen, D. P., 1984a: Mesoscale and convective-scale characteristics of mature hurricanes. Part I: General observations by research aircraft. *J. Atmos. Sci.,* **41,** 1268–1285.

——, 1984b: Mesoscale and convective scale characteristics of mature hurricanes. Part II: Inner core structure of Hurricane Allen (1980). *J. Atmos. Sci.,* **41,** 1287–1311.

Kleinschmidt, E., Jr., 1951: Grundlagen einer Theorie des tropischen Zyklonen. *Arch. Meteor. Geophys. Bioklimatol., Ser. A,* **4,** 53–72.

Koteswaram, P., 1967: On the structure of hurricanes in the upper troposphere and lower stratosphere. *Mon. Wea. Rev.,* **95,** 541–564.

Landsea, C. W., and W. M. Gray, 1994: Northern Hemispheric surface temperature and tropical cyclone activity associations. *Int. J. Climatol.,* in press.

LaSeur, N. E., and H. F. Hawkins, 1963: An analysis of Hurricane Cleo (1958) based on data from research reconnaissance aircraft. *Mon. Wea. Rev.,* **91,** 694–709.

Lighthill, J., G. J. Holland, W. M. Gray, C. Landsea, K. Emanuel, G. Craig, J. Evans, Y. Kurihara, and C. P. Guard, 1994: Global climate change and tropical cyclones. *Bull. Amer. Meteor. Soc.,* **75,** 2147–2157.

Malkus, J. S., 1958: On the structure and maintenance of the mature hurricane eye. *J. Meteor.,* **15,** 337–349.

——, and H. Riehl, 1960: On the dynamics and energy transformations in steady-state hurricanes. *Tellus,* **12,** 1–20.

Marks, F. D., R. A. Houze, and J. F. Gamache, 1992: Dual-aircraft investigation of the inner core of Hurricane Norbert. Part I: Kinematic Structure. *J. Atmos. Sci.,* **49,** 919–942.

Merrill, R. T., 1988: Environmental influences on hurricane intensification. *J. Atmos. Sci.,* **45,** 1678–1687.

——, 1993: Tropical Cyclone Structure. *Global Guide to Tropical Cyclone Forecasting,* WMO/TD-560, G. J. Holland, Ed., World Meteorological Organization, 2.1.1–2.60.

——, and C. S. Velden, 1996: A three-dimensional analysis of the outflow layer of Supertyphoon Flo (1990). *Mon. Wea. Rev.,* **124,** 47–63.

Miller, B. I., 1958: On the maximum intensity of hurricanes. *J. Meteor.,* **15,** 184–195.

Neal, A. B., and G. J. Holland, 1976: The Australian tropical cyclone forecasting manual. 274 pp. [Available from Bureau of Meteorology, P.O. Box 1289K, Melbourne, Victoria 3001, Australia.]

Palmen, E. H., 1948: On the formation and structure of tropical cyclones. *Geophysica,* **3,** 26–38.

Pudov, V. D., and S. A. Petrichenko, 1988: Temperature of the South

China Sea surface and tropical cyclones. *Meteor. Gidrol.,* **12,** 118–121.

Riehl, H., 1948: Aerology of tropical storms. *Compendium of Meteorology,* Amer. Meteor. Soc., 902–913.

——, 1954: *Tropical Meteorology*. McGraw-Hill, 392 pp.

Rotunno, R., and K. A. Emanuel, 1987: An air–sea interaction theory for tropical cyclones, II. *J. Atmos. Sci.,* **44,** 542–561.

Shapiro, L. J., and H. E. Willoughby, 1982: Response of balanced hurricanes to local sources of heat and momentum. *J. Atmos. Sci.,* **39,** 378–394.

Shea, D. J., and W. M. Gray, 1973: The hurricanes's inner core region: Symmetric and asymmetric structure. *J. Atmos. Sci.,* **30,** 1544–1564.

Simpson, R. H., 1952: Exploring the eye of Typhoon Marge, 1951. *Bull Amer. Meteor. Soc.,* **33,** 286–298.

Smith, R. K., 1980: Tropical cyclone eye dynamics. *J. Atmos. Sci.,* **37,** 1227–1232.

Weatherford, C., and W. M. Gray, 1988: Typhoon structure as revealed by aircraft reconnaissance. Part II: Structural variability. *Mon. Wea. Rev.,* **116,** 1044–1056.

Willoughby, H. E., J. A. Clos, and M. G. Shoreibah, 1982: Concentric eyewalls, secondary wind maxima, and the evolution of the hurricane vortex. *J. Appl. Sci.,* **39,** 395–411.